

Fig. 4. Comparison of the envelope proteins and their structural organization in TBEV and HCV. (A) Genomes of TBEV and HCV, with homologous coding domains in the envelope proteins indicated by dotted lines (Yagnik et al., 2000). (B) Structural components of the virus' outer shells: TBEV E-protein dimer and HCV E1–E2 tetramer. (C) Construction of the HCV outer shell from the E1–E2 tetramer. For clarity, only a facet of the icosahedral shell is shown, and the 3- and 5-fold symmetry axes are indicated.

Our model implies that the HCV may share a similar membrane fusion mechanism with other flaviviruses but may differ in its receptor binding. The latter is supported by the observation that the regions of HCV E1 and E2 proteins that are important for receptor interaction are located in the general vicinity of domain III of the flavivirus E protein, which has a similar function (Ferlenghi et al., 2001; Hurrelbrink and McMin, 2001; Kuhn et al., 2002; Mandl et al., 2000; Modis et al., 2003). Contrary to that of flaviviruses, our model of the HCV outer shell organization implies that the infectivity of HCV depends on both the E1 and E2 proteins. Indeed, competition studies with monoclonal antibodies using HCV-LPs and HCV pseudoviruses have shown that the entry of HCV into host cells involves multiple receptors that are recognized by E1 and/or E2. The intricate interactions among E1, E2 and the putative receptor(s) involved in HCV entry await further structural elucidation.

Fitting of the existing model of the dengue virus E protein (Kuhn et al., 2002) into our HCV-LP density map by maximizing the correlation between the cryoEM density and dengue E model (see Materials and methods) revealed a good match between the HCV 'fishbone' structure and the dengue virus E dimers (Fig. 5A). The dengue virus E protein dimer matches well with the density features representing the putative E1–E2 tetramer of HCV-LP, except in the regions around the two ends of the E protein dimers where the flavivirus E protein domain III resides (Fig. 5B). As discussed above, the flavivirus E protein has an immunoglobulin-like domain III that displays a small protrusion on the viral surface. The HCV E1 protein, while structurally replacing this domain III as supported by our localization of the anti-E1 binding site on the HCV-LP (Fig. 3E), lacks such a protruding region.

HCV is distinct from dengue virus and other flaviviruses, at least with respect to the mechanisms of virus assembly and

maturation. Notably, the HCV-LP lacks the M protein layer between the E protein and lipid bilayer. The M protein is believed to play a key role in the transformation of the immature structure, which has surface protrusions, to the mature, smooth-surfaced structure (Allison et al., 2003; Zhang et al., 2003b). Cleavage of the preM by furin causes the dissociation of the preM–E heterodimer and the exposure of the dimerization domain (domain II) of the E protein to form the E homodimer.

Although the assembly of HCV has not been completely elucidated, our findings suggest that the assembly of HCV is generally similar to that of the flaviviruses but with some distinctive features. The HCV E1–E2 heterodimer, which forms in the endoplasmic reticulum during or shortly after translation of the HCV polyprotein, may first assemble into immature viral particles. The heterodimers would then undergo conformational changes to expose the E2 dimerization domains to form dimers of E1–E2 heterodimers leading to the assembly of the outer shell of the mature HCV particle. Unlike flaviviruses, the conformational changes of HCV glycoproteins may occur without proteolytic cleavage, and the E1 and E2 proteins may interact closely during the assembly process, with both proteins located on the surface of the mature virion. In contrast, only E protein is exposed on the outer surface and the mature M protein is buried between the E protein layer and the lipid bilayer in the flaviviruses.

In summary, we have obtained the first 3D model of the HCV particle and obtained direct structural evidence of the external localization of HCV E1. As the first model of a hepacivirus, it reveals key differences and similarities in the structural organization between hepaciviruses and flaviviruses. Further investigation of this model as well as HCV virions isolated from cell culture will provide important insights into

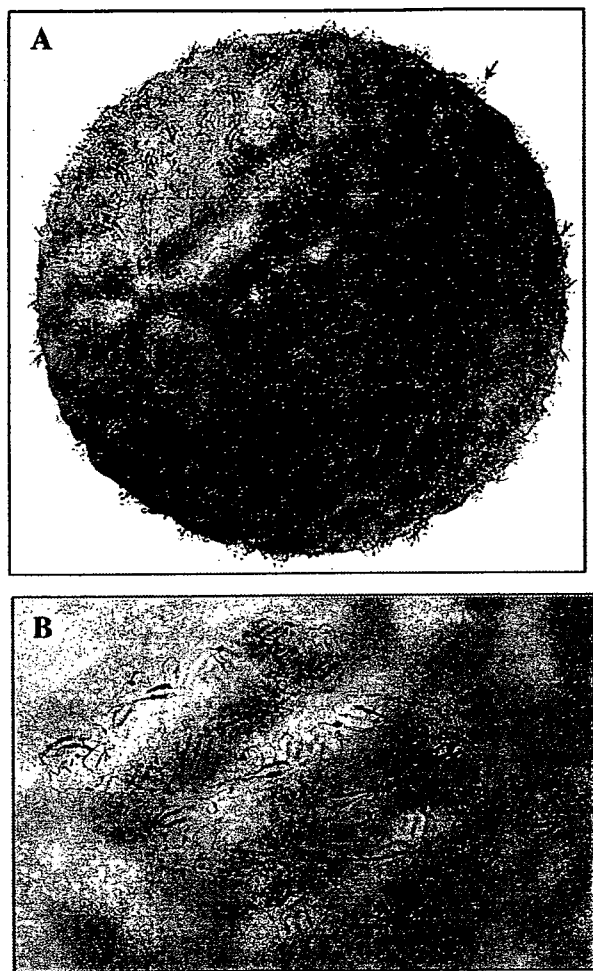


Fig. 5. Fitting of the dengue virus E protein model into the HCV-LP reconstruction. (A) Superposition of the dengue virus E protein model (shown as ribbons) (Kuhn et al., 2002; Modis et al., 2003) over the 3D map of HCV-LP. Five-fold, three-fold and two-fold axes are indicated by '5', '3' and '2', respectively. The arrow indicates the protruding domain III of the dengue virus E protein. (B) Close-up of the region within the dotted line in A. Only three neighboring dengue E-protein dimers are shown for clarity.

the viral assembly and life cycle of HCV. An understanding of the molecular interactions among HCV structural proteins, particularly at higher resolution level, may ultimately reveal novel targets for rational anti-HCV intervention.

Materials and methods

HCV virion purification

JFH-1 HCV virions were produced in cell culture as described previously (Kato et al., 2007; Wakita et al., 2005). The culture medium was first cleared of cellular debris with a 0.45- μm filter. The secreted virions were concentrated by polyethylene glycol 8000 and then subjected to iodixanol density gradient analysis (Heller et al., 2005; Kato et al., 2007). The fractions were examined by negative-stain (2% uranyl acetate) transmission electron microscopy (TEM) and the virion-containing fraction was pelleted and resuspended in

10 mM phosphate-buffered saline (PBS) pH 7.4 for cryoEM imaging.

HCV-LP purification and antibody labeling

HCV-LPs were purified from insect cells infected by recombinant baculoviruses expressing HCV structural proteins (bvHCV.Sp7-) as described (Jeong et al., 2004; Qiao et al., 2004). For antibody labeling, isolated HCV-LPs were incubated with purified mouse monoclonal anti-E1 antibody (E1A4) (from Harry Greenberg, Stanford, CA) at 4 °C for 1 h. The complexes were then subjected to iodixanol density gradient centrifugation (20–50% gradient) in a Beckman SW55 rotor at ~230,000 g for 5 h at 4 °C. Fractions were collected, checked for particle concentration and integrity by negative-stain TEM. Selected HCV-LP-containing fraction was confirmed by Western blot and subsequently resuspended in 10 mM PBS pH 7.4 for cryoEM.

For gold labeling, secondary antibodies conjugated to 10-nm gold particles (KPL, Gaithersburg, MD) were incubated with anti-E1 antibody-labeled HCV-LPs overnight. They were then run through a sucrose gradient to remove unbound secondary antibodies, stained with 2% uranyl acetate and examined by TEM.

CryoEM and 3D reconstruction

CryoEM imaging of HCV-LPs and antibody-labeled HCV-LPs was performed as described previously (Yu et al., 2005; Zhou et al., 2000). Briefly, a 3- μl aliquot of 1.5 mg/ml unlabeled or antibody-labeled HCV-LPs was applied to a Quantifoil R 2/1 grid (Quantifoil Micro Tools GmbH, Jena, Germany), quickly blotted with filter paper and plunged into liquid nitrogen-cooled liquid ethane so that the HCV-LPs or their antibody-labeled complexes were embedded in a thin layer of vitreous ice across the holes of carbon supporting film. Images were recorded at a magnification of 40,000 \times at 100 kV in a JEOL1200 cryo-electron microscope using an electron dose of ~10 electrons/ \AA^2 /micrograph.

For 3D reconstruction, selected micrographs (60 focal pairs for HCV-LP, 67 focal pairs for antibody-labeled HCV-LP) in the proper defocus range and without apparent specimen drift and charging were digitized on a Zeiss SCAI microdensitometer (Z/I Imaging, Huntsville, AL) using a step size equivalent to 7 \AA /pixel on the specimen. Data processing and visualization were carried out on Dell Workstations with Windows XP using Fourier common-lines-based procedures implemented in the IMIRS software package, as previously described (Liang et al., 2002). The defocus values of the micrographs were determined using the incoherently averaged Fourier transforms of particle images. The underfocus values of the micrographs of HCV-LP and antibody-labeled HCV-LP range from 1.5 to 2.8 μm and 1.4 to 2.9 μm , respectively.

Size distribution analysis was carried out by an automatic boxing program (*winBoxer*, Blake Young and Z. H. Zhou, unpublished) using circles with different diameters as templates. We then manually selected 990 HCV-LPs and 432 antibody-labeled HCV-LPs from the 500- \AA group for in-depth iterative

refinement and 3D reconstructions. Most of those particles were eliminated by setting gradually more stringent cut-off value of phase-residues until no improvements of 3D reconstruction were observed as more particles are eliminated. The final 3D reconstructions were generated to 30 Å by merging 110 HCV-LPs or 87 antibody-labeled HCV-LPs. The 3D visualization was performed using Iris Explorer (NAG, Downers Grove, IL) with custom-designed modules and UCSF Chimera (Pettersen et al., 2004). The PDB file with the atomic coordinates of the dengue E protein was downloaded directly from the Protein Data Bank for fitting into our cryoEM structures as described previously (Zhou et al., 2001). Fitting of the atomic model into the cryoEM density map was achieved by using the 'Fit Model in Map' functionality in the UCSF Chimera package, which maximizes the cross correlation between the cryoEM density map and the dengue E protein model.

Acknowledgments

We thank Sook-Hyang Jeong and Miriam Triyatni for assistance and advice and Pierrette Lo for editorial assistance. This research was supported in part by the Intramural Research Program of the National Institute of Diabetes and Digestive and Kidney Diseases.

References

- Allison, S.L., Tao, Y.J., O'Riordain, G., Mandl, C.W., Harrison, S.C., Heinz, F.X., 2003. Two distinct size classes of immature and mature subviral particles from tick-borne encephalitis virus. *J. Virol.* 77, 11357–11366.
- Bartosch, B., Dubuisson, J., Cosset, F.L., 2003. Infectious hepatitis C virus pseudo-particles containing functional E1–E2 envelope protein complexes. *J. Exp. Med.* 197, 633–642.
- Dubuisson, J., 2000. Folding, assembly and subcellular localization of hepatitis C virus glycoproteins. *Curr. Top. Microbiol. Immunol.* 242, 135–148.
- Ferlenghi, I., Clarke, M., Ruttan, T., Allison, S.L., Schalich, J., Heinz, F.X., Harrison, S.C., Rey, F.A., Fuller, S.D., 2001. Molecular organization of a recombinant subviral particle from tick-borne encephalitis virus. *Mol. Cell* 7, 593–602.
- Heller, T., Saito, S., Auerbach, J., Williams, T., Moreen, T.R., Jazwinski, A., Cruz, B., Jeurkar, N., Sapp, R., Luo, G., Liang, T.J., 2005. An in vitro model of hepatitis C virion production. *Proc. Natl. Acad. Sci. U.S.A.* 102, 2579–2583.
- Hurrelbrink, R.J., McMinn, P.C., 2001. Attenuation of Murray Valley encephalitis virus by site-directed mutagenesis of the hinge and putative receptor-binding regions of the envelope protein. *J. Virol.* 75, 7692–7702.
- Jeong, S.H., Qiao, M., Nascimbeni, M., Hu, Z., Rehermann, B., Murthy, K., Liang, T.J., 2004. Immunization with hepatitis C virus-like particles induces humoral and cellular immune responses in nonhuman primates. *J. Virol.* 78, 6995–7003.
- Kanai, R., Kar, K., Anthony, K., Gould, L.H., Ledizet, M., Fikrig, E., Marasco, W.A., Koski, R.A., Modis, Y., 2006. Crystal structure of West Nile virus envelope glycoprotein reveals viral surface epitopes. *J. Virol.* 80, 11000–11008.
- Kato, T., Matsumura, T., Heller, T., Saito, S., Sapp, R.K., Murthy, K., Wakita, T., Liang, T.J., 2007. Production of infectious hepatitis C virus of various genotypes in cell culture. *J. Virol.* 81, 4405–4411.
- Kuhn, R.J., Zhang, W., Rossmann, M.G., Pletnev, S.V., Corver, J., Lenches, E., Jones, C.T., Mukhopadhyay, S., Chipman, P.R., Strauss, E.G., Baker, T.S., Strauss, J.H., 2002. Structure of dengue virus: implications for flavivirus organization, maturation, and fusion. *Cell* 108, 717–725.
- Kunkel, M., Watowich, S.J., 2002. Conformational changes accompanying self-assembly of the hepatitis C virus core protein. *Virology* 294, 239–245.
- Kunkel, M., Lorinczi, M., Rijnbrand, R., Lemon, S.M., Watowich, S.J., 2001. Self-assembly of nucleocapsid-like particles from recombinant hepatitis C virus core protein. *J. Virol.* 75, 2119–2129.
- Liang, T.J., Rehermann, B., Seeff, L.B., Hoofnagle, J.H., 2000. Pathogenesis, natural history, treatment, and prevention of hepatitis C. *Ann. Intern. Med.* 132, 296–305.
- Liang, Y., Ke, E.Y., Zhou, Z.H., 2002. IMIRS: a high-resolution 3D reconstruction package integrated with a relational image database. *J. Struct. Biol.* 137, 292–304.
- Lindenbach, B.D., Evans, M.J., Syder, A.J., Wolk, B., Tellinghuisen, T.L., Liu, C.C., Maruyama, T., Hynes, R.O., Burton, D.R., McKeating, J.A., Rice, C.M., 2005. Complete replication of hepatitis C virus in cell culture. *Science* 309, 623–626.
- Mandl, C.W., Allison, S.L., Holzmann, H., Meixner, T., Heinz, F.X., 2000. Attenuation of tick-borne encephalitis virus by structure-based site-specific mutagenesis of a putative flavivirus receptor binding site. *J. Virol.* 74, 9601–9609.
- Meyer, K., Beyene, A., Bowlin, T.L., Basu, A., Ray, R., 2004. Coexpression of hepatitis C virus E1 and E2 chimeric envelope glycoproteins displays separable ligand sensitivity and increases pseudotype infectious titer. *J. Virol.* 78, 12838–12847.
- Modis, Y., Ogata, S., Clements, D., Harrison, S.C., 2003. A ligand-binding pocket in the dengue virus envelope glycoprotein. *Proc. Natl. Acad. Sci. U.S.A.* 100, 6986–6991.
- Modis, Y., Ogata, S., Clements, D., Harrison, S.C., 2004. Structure of the dengue virus envelope protein after membrane fusion. *Nature* 427 (6972), 313–319.
- Mukhopadhyay, S., Kim, B.S., Chipman, P.R., Rossmann, M.G., Kuhn, R.J., 2003. Structure of West Nile virus. *Science* 302, 248.
- Petit, M.A., Lievre, M., Peyrol, S., De Sequeira, S., Berthillon, P., Ruigrok, R.W., Trepo, C., 2005. Enveloped particles in the serum of chronic hepatitis C patients. *Virology* 336, 144–153.
- Pettersen, E.F., Goddard, T.D., Huang, C.C., Couch, G.S., Greenblatt, D.M., Meng, E.C., Ferrin, T.E., 2004. UCSF chimera—A visualization system for exploratory research and analysis. *J. Comput. Chem.* 25, 1605–1612.
- Pokidysheva, E., Zhang, Y., Battisti, A.J., Bator-Kelly, C.M., Chipman, P.R., Xiao, C., Gregorio, G.G., Hendrickson, W.A., Kuhn, R.J., Rossmann, M.G., 2006. Cryo-EM reconstruction of dengue virus in complex with the carbohydrate recognition domain of DC-SIGN. *Cell* 124, 485–493.
- Prince, A.M., Huima-Byron, T., Parker, T.S., Levine, D.M., 1996. Visualization of hepatitis C virions and putative defective interfering particles isolated from low-density lipoproteins. *J. Viral Hepatitis* 3, 11–17.
- Qiao, M., Ashok, M., Bernard, K.A., Palacios, G., Zhou, Z.H., Lipkin, W.I., Liang, T.J., 2004. Induction of sterilizing immunity against West Nile virus (WNV), by immunization with WNV-like particles produced in insect cells. *J. Infect. Dis.* 190, 2104–2108.
- Rey, F.A., Heinz, F.X., Mandl, C., Kunz, C., Harrison, S.C., 1995. The envelope glycoprotein from tick-borne encephalitis virus at 2 Å resolution. *Nature* 375, 291–298.
- Trestard, A., Bacq, Y., Buzelay, L., Dubois, F., Barin, F., Goudeau, A., Roingard, P., 1998. Ultrastructural and physicochemical characterization of the hepatitis C virus recovered from the serum of an agammaglobulinemic patient. *Arch. Virol.* 143, 2241–2245.
- Triyatni, M., Saunier, B., Maruvada, P., Davis, A.R., Ulianich, L., Heller, T., Patel, A., Kohn, L.D., Liang, T.J., 2002a. Interaction of hepatitis C virus-like particles and cells: a model system for studying viral binding and entry. *J. Virol.* 76, 9335–9344.
- Triyatni, M., Vergalla, J., Davis, A.R., Hadlock, K.G., Fong, S.K., Liang, T.J., 2002b. Structural features of envelope proteins on hepatitis C virus-like particles as determined by anti-envelope monoclonal antibodies and CD81 binding. *Virology* 298, 124–132.
- Wakita, T., Pietschmann, T., Kato, T., Date, T., Miyamoto, M., Zhao, Z., Murthy, K., Habermann, A., Krausslich, H.G., Mizokami, M., Bartenschlager, R., Liang, T.J., 2005. Production of infectious hepatitis C virus in tissue culture from a cloned viral genome. *Nat. Med.* 11, 791–796.
- Yagnik, A.T., Lahm, A., Meola, A., Roccasecca, R.M., Ercole, B.B., Nicosia, A., Tramontano, A., 2000. A model for the hepatitis C virus envelope glycoprotein E2. *Proteins* 40, 355–366.
- Yu, X., Shah, S., Atansov, I., Lo, P., Liu, F., Britt, W.J., Zhou, Z.H., 2005.

- Three-dimensional localization of the smallest capsid protein in the human cytomegalovirus capsid. *J. Virol.* 79, 1327–1332.
- Zhang, W., Chipman, P.R., Corver, J., Johnson, P.R., Zhang, Y., Mukhopadhyay, S., Baker, T.S., Strauss, J.H., Rossmann, M.G., Kuhn, R.J., 2003a. Visualization of membrane protein domains by cryo-electron microscopy of dengue virus. *Nat. Struct. Biol.* 10, 907–912.
- Zhang, Y., Corver, J., Chipman, P.R., Zhang, W., Plenev, S.V., Sedlak, D., Baker, T.S., Strauss, J.H., Kuhn, R.J., Rossmann, M.G., 2003b. Structures of immature flavivirus particles. *EMBO J.* 22, 2604–2613.
- Zhong, J., Gastaminza, P., Cheng, G., Kapadia, S., Kato, T., Burton, D.R., Wieland, S.F., Uprichard, S.L., Wakita, T., Chisari, F.V., 2005. Robust hepatitis C virus infection in vitro. *Proc. Natl. Acad. Sci. U.S.A.* 102, 9294–9299.
- Zhou, Z.H., Dougherty, M., Jakana, J., He, J., Rixon, F.J., Chiu, W., 2000. Seeing the herpesvirus capsid at 8.5 Å. *Science* 288, 877–880.
- Zhou, Z.H., Liao, W., Cheng, R.H., Lawson, J.E., McCarthy, D.B., Reed, L.J., Stoops, J.K., 2001. Direct evidence for the size and conformational variability of the pyruvate dehydrogenase complex revealed by three-dimensional electron microscopy. The “breathing” core and its functional relationship to protein dynamics. *J. Biol. Chem.* 276, 21704–21713.

The NS3 Helicase and NS5B-to-3'X Regions Are Important for Efficient Hepatitis C Virus Strain JFH-1 Replication in Huh7 Cells[∇]

Asako Murayama,¹ Tomoko Date,¹ Kenichi Morikawa,¹ Daisuke Akazawa,^{1,2} Michiko Miyamoto,³ Minako Kaga,¹ Koji Ishii,¹ Tetsuro Suzuki,¹ Takanobu Kato,^{4,5} Masashi Mizokami,⁴ and Takaji Wakita^{1*}

Department of Virology II, National Institute of Infectious Diseases, Tokyo, Japan¹; Pharmaceutical Research Lab, Toray Industries, Inc., Kanagawa, Japan²; Department of Microbiology, Tokyo Metropolitan Institute for Neuroscience, Tokyo, Japan³; Department of Clinical Molecular Informative Medicine, Nagoya City University Graduate School of Medical Sciences, Nagoya, Japan⁴; and Liver Disease Branch, NIDDK, National Institutes of Health, Bethesda, Maryland⁵

Received 23 September 2006/Accepted 8 May 2007

The JFH-1 strain of hepatitis C virus (HCV) is a genotype 2a strain that can replicate autonomously in Huh7 cells. The J6 strain is also a genotype 2a strain, but its full genomic RNA does not replicate in Huh7 cells. However, chimeric J6/JFH-1 RNA that has J6 structural-protein-coding regions and JFH-1 nonstructural-protein-coding regions can replicate autonomously and produce infectious HCV particles. In order to determine the mechanisms underlying JFH-1 RNA replication, we constructed various J6/JFH-1 chimeras and tested their RNA replication and virus particle production abilities in Huh7 cells. Via subgenomic-RNA-replication assays, we found that both the JFH-1 NS5B-to-3'X (NSBX) and the NS3 helicase (N3H) regions are important for the replication of the J6CF replicon. We applied these results to full-length genomic RNA replication and analyzed replication using Northern blotting. We found that a chimeric J6 clone with JFH-1 N3H and NSBX could replicate autonomously but that a chimeric J6 clone with only JFH-1 NSBX had no replication ability. Finally, we tested the virus production abilities of these clones and found that a chimeric J6 clone with JFH-1 N3H and NSBX could produce infectious HCV particles. In conclusion, the JFH-1 NS3 helicase and NS5B-to-3'X regions are important for efficient replication and virus particle formation of HCV genotype 2a strains.

Hepatitis C virus (HCV) is a major cause of chronic liver disease (7, 22). The lack of a robust cell culture system for producing virus particles has hampered the development of HCV research (2). Although the development of a subgenomic-replicon system enabled research into HCV RNA replication (32), infectious-virus-particle production remained impossible. Recently, an HCV cell culture system was developed using a JFH-1 genotype 2a strain of HCV cloned from a fulminant hepatitis patient (30, 48, 54), allowing investigation of the virus life cycle.

HCV is a positive-strand RNA virus that belongs to the *Hepacivirus* genus in the *Flaviviridae* family. The HCV genome comprises about 9,600 nucleotides that encode a single polyprotein of around 3,000 amino acids (8, 18, 44), which is processed by cellular and viral encoded proteases into at least 10 different structural and nonstructural proteins (11, 13, 14, 33).

The JFH-1 strain of HCV is a genotype 2a strain, and it is the first HCV strain that can produce HCV particles in Huh7 cells (48). Subgenomic replicons of JFH-1 replicate efficiently in Huh7 cells and do not require cell culture-adaptive mutations (19). The J6CF strain of HCV is also a genotype 2a strain and is known to be infectious in chimpanzees (49), but its

entire genomic RNA does not replicate in Huh7 cells, despite the ~90% nucleotide sequence homology between JFH-1 and J6CF. However, J6/JFH-1 chimeric RNA that has J6 structural-protein-coding regions and JFH-1 nonstructural-protein-coding regions can replicate autonomously and produce infectious HCV particles (30, 39). Why only the JFH-1 clone can replicate efficiently in Huh7 cells remains unclear.

In this study, to investigate the mechanisms underlying efficient JFH-1 replication, we focused on the differences in replication between JFH-1 and J6CF strains by using intragenotypic JFH-1 and J6CF chimeras and compared their respective abilities to replicate RNA and produce virus particles in Huh7 cells.

MATERIALS AND METHODS

Cell culture. Huh7 cells (36) were cultured at 37°C in Dulbecco's modified Eagle's medium containing 10% fetal bovine serum under 5% CO₂ conditions.

Subgenomic-replicon constructs. pSGR-JCH1 and pSGR-JCH4 were constructed based on pSGR-JFH1 (19, 21). pSGR-J6CF was also constructed from pJ6CF (a kind gift from Jens Bukh) (49), using the same method used to construct pSGR-JFH1. Plasmids used in luciferase assays were constructed based on pSGR-JFH1/Luc (20). Chimeric replicons were constructed by substitution of the corresponding regions. For convenience, several restriction enzyme recognition sites (ClaI [2275], EcoT22I [3639], and BsrGI [6127]) were introduced into the pSGR-J6CF sequence via nucleotide substitutions. The substitutions of the corresponding regions were achieved as follows, with the 5' untranslated region (5'UTR) inserted between NotI and AgeI: NS3, PmeI-EcoT22I; NS3 protease, PmeI-ClaI; NS3 helicase, ClaI-EcoT22I; NS4, EcoT22I-MunI; NS5A, MunI-BsrGI; NS5B, BsrGI-StuI; and 3'UTR, StuI-XbaI (see Fig. 2A and 3A). pSGR-JCH1/Luc and pSGR-JCH4/Luc were also constructed using the same procedure as that for pSGR-JFH1/Luc (20, 21). The Con1 replicon (pSGR-Con1/Luc) was

* Corresponding author. Mailing address: Department of Virology II, National Institute of Infectious Diseases, Toyama 1-23-1, Shinjuku, Tokyo 162-8640, Japan. Phone: 81-3-5285-1111. Fax: 81-3-5285-1161. E-mail: wakita@nih.go.jp.

[∇] Published ahead of print on 23 May 2007.

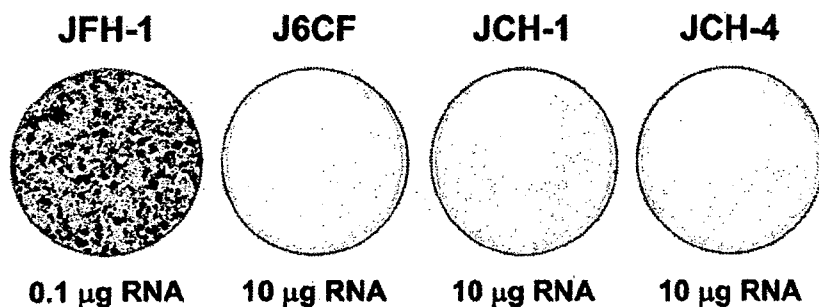


FIG. 1. G418-resistant colony formation of JFH-1, J6CF, JCH-1, and JCH-4. Subgenomic RNAs were synthesized *in vitro*, using pSGR-JFH1, pSGR-J6CF, pSGR-JCH1, and pSGR-JCH4 as templates. Transcribed subgenomic RNAs were electroporated into Huh7 cells, and cells were cultured with G418 for 3 weeks before staining with crystal violet as described in Materials and Methods. JFH-1 subgenomic RNA (0.1 μ g) and 10 μ g of J6CF, JCH-1, and JCH-4 subgenomic RNAs were transfected into Huh7 cells. Experiments were performed in triplicate, and representative staining examples are shown.

constructed from pFK-1389/neo/NS3-3'/wt (a kind gift from Ralf Bartenschlager) (32), and the H77c replicon (pSGR-H77c/Luc) was constructed from pCV-H77c (a kind gift from Robert H. Purcell) (50). For convenience, ClaI (2275) and BsrGI (6127) recognition sites were introduced into the pSGR-Con1/Luc and pSGR-H77c/Luc sequences via nucleotide substitutions. Substitutions of the NS3 helicase region and NS5B regions were performed as described above.

Full-length genomic HCV constructs. Plasmids used in the analysis of genomic RNA replication were constructed based on pJFH1 (48) and pJ6CF (49). For convenience, several restriction enzyme recognition sites (ClaI [3929], EcoT22I [5293], and BsrGI [7781]) were introduced into the J6CF sequence via nucleotide substitutions. Substitutions of the NS3 helicase regions were performed by replacement of the ClaI-EcoT22I fragment, substitutions of the NS5B regions were performed by replacement of the BsrGI-XbaI fragment, substitutions of the NS5A regions were performed by replacement of the BsrGI-StuI fragment, and a substitution of the 3'UTR was performed by replacement of the StuI-XbaI fragment (see Fig. 5A).

RNA synthesis and transfection. RNA synthesis and transfection were performed as described previously (48). In brief, plasmids were linearized with XbaI, treated with mung bean nuclease (New England Biolabs, Ipswich, MA), and purified. Linearized, purified DNAs were used as templates for *in vitro* RNA synthesis using a MEGAscript T7 kit (Ambion, Austin, TX) in accordance with the manufacturer's instructions. Synthesized RNA was treated with DNase I (Ambion), followed by purification using ISOGEN-LS (Nippon Gene, Tokyo, Japan). The quality of synthesized RNA was examined by agarose gel electrophoresis. Ten micrograms of *in vitro*-synthesized RNA was used for each electroporation. Trypsinized Huh7 cells (3×10^6 cells) were washed with Opti-MEM I (Invitrogen, Carlsbad, CA) and resuspended in Cytomix buffer (47). RNA was mixed with 400 μ l of cell suspension, and the mixture was then transferred to an electroporation cuvette (Precision Universal Cuvettes, Thermo Hybaid, Middlesex, United Kingdom). The cells were then pulsed at 260 V and 950 μ F using a Gene Pulser II apparatus (Bio-Rad, Hercules, CA). Transfected cells were immediately transferred to 10-cm culture dishes or six-well plates, each containing culture medium, and incubated at 37°C under 5% CO₂. Luciferase mRNA was synthesized from luciferase T7 control DNA (Promega, Madison, WI) by using a mMESAGE mMACHINE T7 kit (Ambion). To monitor transfection efficiency, *in vitro*-synthesized luciferase RNA was cotransfected with HCV RNA and luciferase activity measured at 4 h after transfection.

G418-resistant colony formation assay. The G418-resistant colony formation assay was performed as described previously (19). In brief, 0.1 μ g or 10 μ g of transcribed RNAs was transfected into 3×10^6 Huh7 cells by electroporation. Transfected cells were immediately transferred to 10-cm culture dishes containing 10 ml of culture medium. G418 (1.0 mg/ml) (Nakalai Tesque, Kyoto, Japan) was added to the culture medium at 16 to 24 h after transfection. Culture medium supplemented with G418 was replaced every 3 days. Three weeks after transfection, cells were fixed with buffered formalin and stained with crystal violet.

Luciferase reporter assay. The luciferase activities of the JFH-1 subgenomic replicon and chimeras in Huh7 cells were measured as described previously (20). Briefly, 5 μ g of transcribed RNAs was transfected into 3×10^6 Huh7 cells by electroporation. Transfected cells were immediately resuspended in culture medium and seeded into six-well culture plates. Cells were harvested serially at 4, 24, and 48 h after transfection and lysed with 200 μ l of cell culture lysis reagent

(Promega). Debris was then removed by centrifugation. Luciferase activity was quantified using a Lumat LB9507 luminometer (EG & G Berthold, Bad Wildbad, Germany) and a luciferase assay system (Promega). Assays were performed three times independently, with each value corrected for transfection efficiency as determined by measuring luciferase activity 4 h after transfection. The data are expressed as relative luciferase units (RLU).

Quantification of HCV core protein. To estimate the concentration of HCV core protein in the culture medium, we performed an HCV core enzyme-linked immunosorbent assay (Ortho-Clinical Diagnostics, Tokyo, Japan) in accordance with the manufacturer's instructions.

Northern blot analysis. Northern blot analysis was performed as described previously (48). In brief, total cellular RNA from HCV RNA-transfected cells was extracted using ISOGEN (Nippon Gene) in accordance with the manufacturer's instructions. Isolated RNA (2 μ g) was separated on a 1% agarose gel containing formaldehyde, transferred to a Hybond N+ positively charged nylon membrane (GE Healthcare, Piscataway, NJ), and immobilized using a Stratalkink UV cross-linker (Stratagene, La Jolla, CA). Hybridization was performed with [α -³²P]dCTP-labeled DNA by using Rapid-Hyb buffer (GE Healthcare). The DNA probe was synthesized using the NSSB-to-3'X fragment of JFH1 excised from pJFH1 by BsrGI and XbaI and labeled using the Megaprime DNA labeling system (GE Healthcare).

Infection of cells with secreted HCV and determination of infectivity. Culture medium from RNA-transfected cells was collected at 72 h posttransfection. Huh7 cells were seeded at a density of 1×10^4 cells per well in poly-D-lysine-coated 96-well plates (CORNING, Corning, NY). On the following day, the collected culture media were serially diluted and used for inoculation of the seeded cells, and the plates were incubated for another 3 days at 37°C. The cells were fixed in methanol for 15 min at -20°C, and the infected foci were visualized by immunofluorescence as described below.

Cells were blocked for 1 h with BlockAce (Dainippon Sumitomo Pharma, Osaka, Japan) supplemented with 0.3% Triton X-100 and then washed with phosphate-buffered saline, followed by incubation with anti-core antibody at 50 μ g/ml in BlockAce. After incubation for 1 h at room temperature, the cells were washed and incubated with a 1:400 dilution of AlexaFluor 488-conjugated anti-mouse immunoglobulin G (Molecular Probes, Eugene, OR) in BlockAce. The cells were then washed and examined using fluorescence microscopy (Olympus, Tokyo, Japan). Infectivity was quantified by counting the infected foci and expressed as numbers of focus-forming units per milliliter (FFU/ml).

RESULTS

G418-resistant colony formation of JFH-1, J6CF, and other genotype 2a subgenomic replicons. First, to compare the replication efficiencies of the JFH-1 and J6CF strains, we performed a G418-resistant colony formation assay with JFH-1 and J6CF RNAs by using subgenomic replicons. The JFH-1 subgenomic replicon formed many colonies with transfection of only 0.1 μ g RNA, but the J6CF subgenomic replicon formed no colonies, even with transfection of 10 μ g RNA (Fig. 1). We also tested

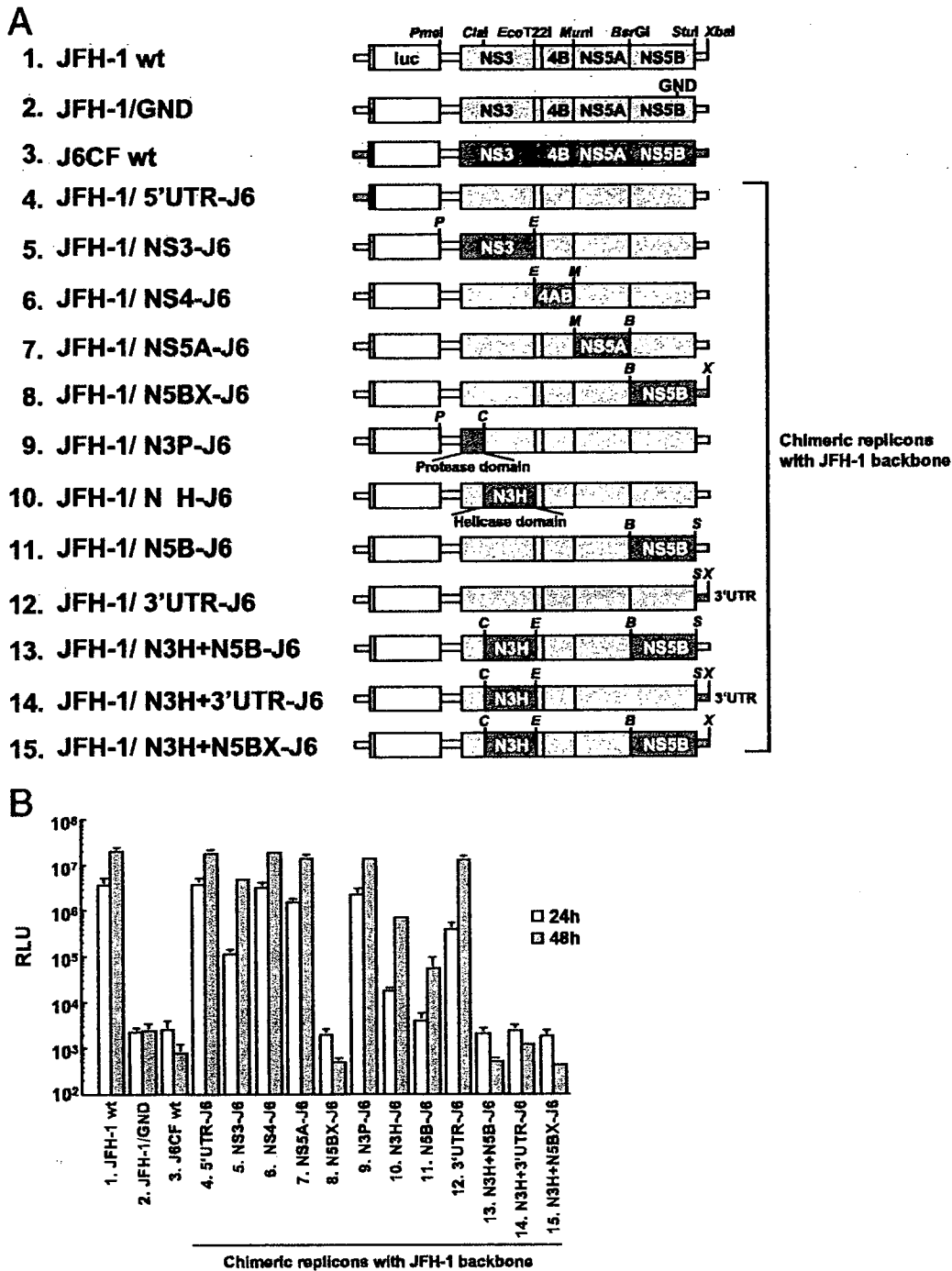


FIG. 2. Luciferase activities of chimeric replicons with a JFH-1 backbone. (A) Structures of chimeric subgenomic replicons with a JFH-1 backbone. The restriction enzyme recognition sites used for the construction of plasmids are indicated. P, PmeI; C, ClaI; E, EcoT22I; M, MunI; B, BsrGI; S, StuI; X, XbaI; wt, wild type. (B) Subgenomic RNAs were synthesized in vitro from wild-type or chimeric replicon constructs. Transcribed subgenomic RNAs (5 μ g) were electroporated into Huh7 cells, and cells were harvested serially at 4, 24, and 48 h after transfection. The harvested cells were lysed, and then luciferase activities in the cell lysates were measured. The assays were performed three times independently and the results expressed as luciferase activities (RLU). Each value was corrected for transfection efficiency as determined by measuring the luciferase activity 4 h after transfection. Data are presented as means and standard deviations for luciferase activity at 24 h (white bars) and 48 h (gray bars) after transfection.

other genotype 2a clones (the JCH-1 and JCH-4 strains), which were isolated from patients with chronic hepatitis C (21). Their subgenomic replicons did not form colonies either. Given that chimeric J6/JFH-1 RNA that has the J6 structural-protein-coding

regions and JFH-1 nonstructural-protein-coding regions reportedly replicates autonomously and produces infectious HCV particles (30, 39), we hypothesized that some of the JFH-1 nonstructural-protein-coding regions are important for JFH-1 replication.

Regions of JFH-1 essential for replication. In order to determine which regions of JFH-1 are important for JFH-1 RNA replication, we constructed a series of chimeric JFH-1 subgenomic replicons replacing the 5'UTR, NS3, NS4AB, NS5A, and NS5B-to-3'X (N5BX) regions from the J6CF strain and tested their replication abilities. For this analysis, we adopted luciferase replicon systems (20) because colony formation assays are time-consuming to perform and it is difficult to evaluate precise replication levels using this method. Furthermore, efficient JFH-1 RNA replication may reduce cellular growth, thus affecting colony formation efficiency (34). We constructed JFH-1 chimeric subgenomic luciferase replicons with the J6CF clone because this clone was reportedly infectious in a chimpanzee (49). However, the JCH-1 and JCH-4 clones were not tested for infectivity. The 5'UTR, NS3, NS4AB, NS5A, or N5BX sequences of the JFH-1 replicon were replaced by J6CF sequences (5'UTR-J6, NS3-J6, NS4-J6, NS5A-J6, or N5BX-J6, respectively [Fig. 2A]). The luciferase activities of these replicons are shown in Fig. 2B. The JFH-1 subgenomic replicon replicated efficiently and had a luciferase activity of approximately 10^7 RLU (Fig. 2B, JFH-1 wt). GND, which was replication incompetent because of a mutation at the GDD motif in the NS5B region, had a luciferase activity of only 10^3 RLU (Fig. 2B, JFH-1/GND), which was taken as the background level. The J6CF subgenomic replicon did not replicate and had the same luciferase activity as GND (Fig. 2B, J6CF wt). Replacement of the 5'UTR, NS4AB, and NS5A sequences of JFH-1 by J6CF sequences (5'UTR-J6, NS4-J6, and NS5A-J6, respectively) did not reduce replication (Fig. 2B, 5'UTR-J6 and NS4-J6) or reduced it only slightly (Fig. 2B, NS5A-J6). However, there was no replication for the JFH-1 chimera with J6 N5BX (Fig. 2B, N5BX-J6). In addition, the JFH-1 chimera with the J6 NS3 region (NS3-J6) had a replication level that was more than 10-fold lower at 24 h and around 10-fold lower at 48 h than that of the wild-type JFH-1 replicon (Fig. 2B, JFH-1 wt and NS3-J6). These data show that the JFH-1 NS5B-to-3'X region is essential for JFH-1 RNA replication and indicate that the JFH-1 NS3 region is also important for JFH-1 RNA replication.

Involvement of the NS3 helicase region in efficient JFH-1 replication. The JFH-1 chimera with the J6 NS3 region (NS3-J6) reduced the replication level (Fig. 2B, NS3-J6). The NS3 protein is known to have two domains: a protease domain at the amino terminal one-third and a helicase domain at the carboxyl terminal two-thirds. To determine which region is important for replication, we compared the replication activity of a JFH-1 chimera with that of the NS3 protease-coding region of J6CF (N3P-J6) and that of a JFH-1 chimera with that of the NS3 helicase-coding region of J6CF (N3H-J6) (Fig. 2A, JFH-1/N3P-J6 and JFH-1/N3H-J6). Although N3P-J6 had the same luciferase activity as JFH-1, N3H-J6 had lower activity than JFH-1 (Fig. 2B, N3P-J6 and N3H-J6). These data show that the JFH-1 NS3 helicase-coding region has an important role in JFH-1 replication.

Importance of the JFH-1 NS5B-coding region and 3'UTR in replication. The JFH-1 chimera with J6 N5BX completely abolished replicon replication (Fig. 2B, N5BX-J6). The N5BX region contains two regions, the NS5B protein-coding region and the 3'UTR. The NS5B protein-coding region encodes RNA-dependent RNA polymerase. To analyze which region of

N5BX is important for replication, we separated N5BX into two regions, that is, the NS5B-coding region and the 3'UTR. JFH-1 replicons with NS5B or with the 3'UTR of J6 were constructed (Fig. 2A, JFH-1/N5B-J6 and JFH-1/3'UTR-J6) and their replication abilities analyzed. The replication level of JFH-1/N5B-J6 was reduced more than 100-fold compared with that of the wild-type JFH-1 replicon at 48 h (Fig. 2B, N5B-J6). JFH-1/3'UTR-J6 replicated similarly to JFH-1 at 48 h, but the replication activity at 24 h was reduced more than 10-fold compared with that of the original JFH-1 replicon (Fig. 2B, 3'UTR-J6). These data indicate that the NS5B-coding region and the 3'UTR of JFH-1 are both involved in efficient JFH-1 replication.

Rescue of J6CF replicon replication by incorporation of the JFH-1 sequences. Because the JFH-1 N5BX region appeared to be essential for JFH-1 replication (Fig. 2B, N5BX-J6), we tested whether JFH-1 N5BX could restore the replication of J6CF RNA. We constructed a chimeric J6CF subgenomic replicon containing the JFH-1 N5BX region (Fig. 3A, J6/N5BX-JFH1) and tested its replication abilities. The luciferase activity of J6CF subgenomic RNA was recovered by inclusion of JFH-1 N5BX (Fig. 3B, N5BX-JFH1), but this chimeric replicon showed lower replication activity than the original JFH-1 replicon (Fig. 3B, JFH-1 wt). Furthermore, J6CF replication was not restored by only JFH-1 NS5B (J6/N5B-JFH1) or only the 3'UTR (J6/3'UTR-JFH1) (Fig. 3B, N5B-JFH1 or 3'UTR-JFH1, respectively). These observations clearly indicate that the JFH-1 NS5B-to-3'X region is essential, and the NS5B-coding region and 3'UTR are both important for efficient RNA replication in Huh7 cells. However, other JFH-1 regions are also involved in efficient replication.

The JFH-1 NS3 helicase-coding region was also important for efficient replication, and we thus tested whether the JFH-1 NS3 helicase region by itself could restore J6CF replication (as occurred for the JFH-1 N5BX region). Insertion of only the NS3 helicase region of JFH-1 into J6CF (Fig. 3A, J6/N3H-JFH1) did not restore replication (Fig. 3B, N3H-JFH1). However, replication of the J6 chimeric replicon seemed considerably restored by insertion of JFH-1 NS5B or the 3'UTR in addition to the NS3 helicase-coding region (Fig. 3B, N3H+N5B-JFH-1 or N3H+3'UTR-JFH-1, respectively) and fully restored by insertion of the JFH-1 NS3 helicase region and JFH-1 N5BX region (Fig. 3B, N3H+N5BX-JFH1). These results indicate that the JFH-1 N5BX region is essential for subgenomic-replicon replication and that the JFH-1 NS3 helicase-coding region has an additional role in replication. This was also confirmed by analysis of the replication abilities of JFH-1 replicons with double substitutions of J6CF (Fig. 2A, JFH-1/N3H+N5B-J6, JFH-1/N3H+3'UTR-J6, and JFH-1/N3H+N5BX-J6). Neither of these chimeric JFH-1 replicons replicated (Fig. 2B, N3H+N5B-J6, N3H+3'UTR-J6, and N3H+N5BX-J6).

The NS3 helicase and NS5B-3'X regions of JFH-1 can restore the replication of other genotype 2a replicons but not of genotype 1 replicons. To test whether the JFH-1 NS3 helicase and N5BX regions could restore other HCV replicon replication, chimeric replicon constructs N3H-JFH1, N5BX-JFH1, and N3H+N5BX-JFH1 were constructed using two genotype 2a replicons (JCH-1 and JCH-4), a genotype 1a replicon (H77c), and a genotype 1b replicon (Con1), respectively. The

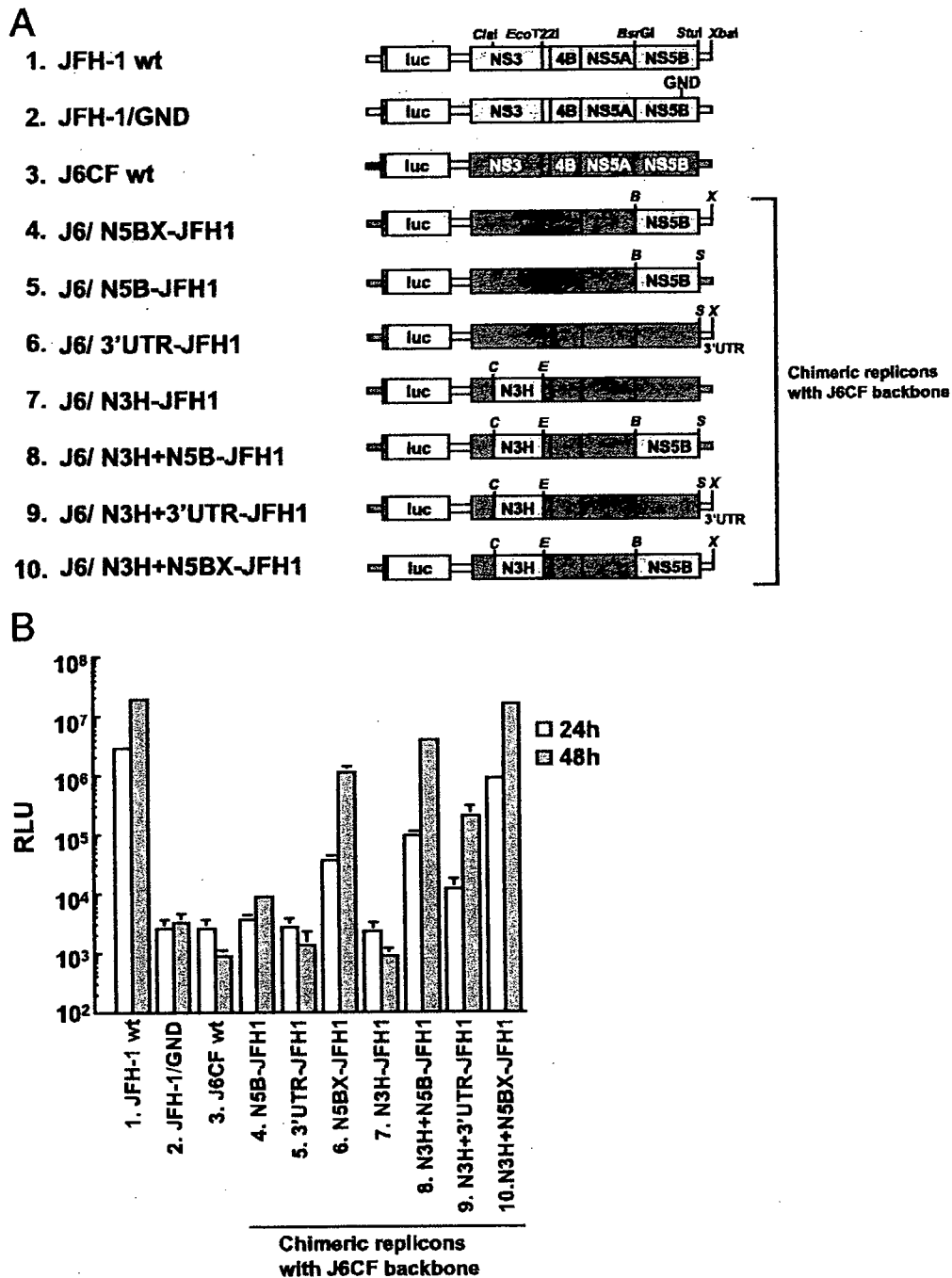


FIG. 3. Luciferase activities of chimeric replicons with a J6CF backbone. (A) Structures of chimeric subgenomic replicons with a J6CF backbone. The restriction enzyme recognition sites used for the construction of plasmids are indicated. C, ClaI; E, EcoT22I; B, BsrGI; S, StuI; X, XbaI; wt, wild type. (B) Wild-type or chimeric subgenomic RNAs were transfected into Huh7 cells, and the luciferase activities of the transfected cells were examined as described in the legend to Fig. 2B. Assays were performed three times independently, and data are presented as means and standard deviations for luciferase activity (RLU) at 24 h (white bars) and 48 h (gray bars) after transfection.

replication level of each wild-type and chimeric replicon was evaluated by luciferase activity measurement after transient transfection of replicon RNA. No replication of any of the wild-type replicons (Fig. 4, JCH-1 wt, JCH-4 wt, H77c wt, and Con1 wt) or of any of the replicons with insertion of the JFH-1 NS3 helicase region (Fig. 4, JCH-1/N3H-JFH1, JCH-4/N3H-

JFH1, H77c/N3H-JFH1, and Con1/N3H-JFH1) was detected. However, genotype 2a replicons with insertion of the JFH-1 N5BX region increased their replication levels severalfold at 48 h (Fig. 4, JCH-1/N5BX-JFH1 and JCH-4/N5BX-JFH1). Furthermore, insertion of both the N3H and the N5BX regions increased the JCH-1 replication over 10-fold compared to that

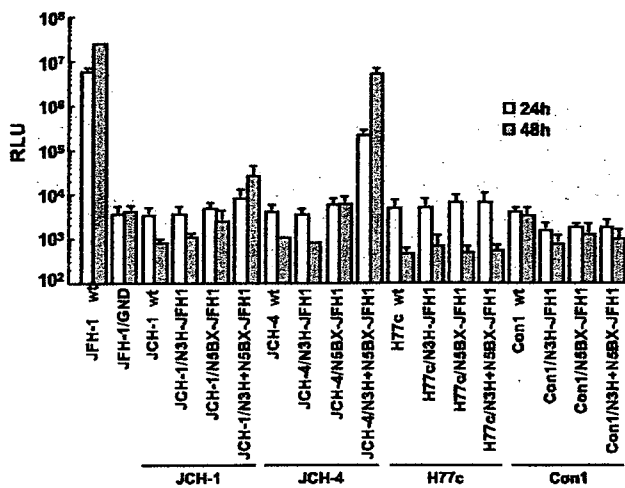


FIG. 4. Restoration of genotype 2a and genotype 1 replicon replication by the insertion of JFH-1 sequences. Two genotype 2a replicons, JCH-1 and JCH-4, a genotype 1a replicon, H77c, and a genotype 1b replicon, Con-1, were used in this assay. Three kinds of chimeric replicons, N3H-JFH-1, N5BX-JFH1, and N3H+N5BX-JFH-1, were prepared for all four HCV replicons. Wild-type (wt) or chimeric subgenomic RNAs were transfected into Huh7 cells and the luciferase activities of the transfected cells examined as described in the legend to Fig. 2B. The assays were performed three times independently, and data are presented as means and standard deviations for luciferase activity (RLU) at 24 h (white bars) and 48 h (gray bars) after transfection.

of wild-type JCH-1 at 48 h and recovered the JCH-4 replication to a level similar to that of wild-type JFH-1 at 48 h (Fig. 4, JCH-1/N3H+N5BX-JFH1 and JCH-4/N3H+N5BX-JFH1, respectively). On the other hand, insertion of the JFH-1 N5BX region or both the N3H and the N5BX regions did not restore H77c or Con1 replicon replication (Fig. 4, H77c/N5BX-JFH1, H77c/N3H+N5BX-JFH1, Con1/N5BX-JFH1, and Con1/N3H+N5BX-JFH1). HCV polyprotein processing is critically important for HCV RNA replication and virus production, and this processing may be affected by the chimeric RNA molecules between different isolates of genotype 2 as well as those between genotypes 1 and 2. However, our data indicated that HCV polyprotein processing did not differ among the chimeric constructs (data not shown). Thus, the JFH-1 N3H and N5BX regions can rescue the replication of genotype 2a replicons at different levels but not the replication of genotype 1 replicons.

The NS3 helicase and NS5B-3'X regions are both important for JFH-1 genomic RNA replication. Next, we applied the previously described results to genomic RNA replication. The structures of HCV, the template DNA for JFH-1, and the chimeric full-genomic RNAs are shown in Fig. 5A. Full-length HCV RNAs were synthesized as described above and their quality and integrity then confirmed by gel electrophoresis (data not shown). To analyze the transient RNA replication of these chimeric RNAs in Huh7 cells, the synthesized RNAs were transfected into Huh7 cells and total RNA was extracted from HCV RNA-transfected cells at various time points. Northern blot analysis was then performed. The equality of the transfection efficiencies was confirmed by the cotransfection of luciferase mRNA (data not shown). As shown in Fig. 5B, JFH-1 RNA decreased at 10 h after transfection but replicated

efficiently at 24 to 48 h after transfection, as described previously (48). J6 chimeric RNA with the NS3 helicase and N5BX regions of JFH-1 (J6/N3H+N5BX-JFH1) replicated with similar kinetics but with lower efficiency. J6 chimeric RNA with JFH-1 N5BX (J6/N5BX-JFH1) showed no replication in this assay, like J6CF or JFH-1 GND, although this chimera replicated to a considerable extent in subgenomic-replicon assays. Taken together, these data indicate that the NS3 helicase-coding region and the NS5B-to-3'X region of JFH-1 are both essential for full-length genomic HCV RNA replication in Huh7 cells.

Core protein and infectious-chimeric-virus secretion from chimeric J6CF RNA-transfected cells. Finally, we tested whether chimeric RNA-transfected cells could secrete infectious virus particles. Figure 5C shows the core protein secretion into the culture medium from JFH-1, JFH-1/GND, J6CF, and chimeric-RNA-transfected cells. Core protein was efficiently secreted from cells transfected with JFH-1 RNA (Fig. 5C and Table 1) and those transfected with J6/N3H+N5BX-JFH1 RNA, but with efficiencies lower than that for JFH-1 (Fig. 5C and Table 1). J6/N5BX-JFH1, JFH-1/GND, and J6CF RNA-transfected cells, which showed no RNA replication by Northern blot analysis (Fig. 5B), did not secrete core proteins into the culture medium (Table 1). By the replicon assay, JFH-1/N5BX-J6 showed no replication in Huh7 cells (Fig. 2B, N5BX-J6), and full-length JFH-1/N5BX-J6 RNA-transfected cells did not secrete core protein into the culture medium (Table 1). On the other hand, JFH-1/N5B-J6 replicated to some extent in the replicon assay (Fig. 2B, N5B-J6), and full-length JFH-1/N5B-J6 RNA-transfected cells secreted a smaller amount of core protein than JFH-1 RNA-transfected cells (Fig. 5C and Table 1). Both JFH-1/N3H-J6 and JFH-1/3'UTR-J6 RNA-transfected cells secreted about half the amount of core protein that the JFH-1 RNA-transfected cells did (Fig. 5C and Table 1); however, the replication level of the JFH-1/N3H-J6 replicon was markedly lower than those of the JFH-1 and JFH-1/3'UTR-J6 replicons (Fig. 2B, JFH-1 wt, N3H-J6, and 3'UTR-J6), and the replication level of full-length JFH-1/N3H-J6 RNA was also lower than those of the JFH-1 and JFH-1/3'UTR-J6 RNAs as determined by Northern blot analysis (data not shown). Transfection of the other two chimeric RNAs, JFH-1/N3H+N5B-J6 and JFH-1/N3H+N5BX-J6, did not induce core protein secretion (Table 1), and this is in agreement with the finding that neither chimeric replicon replicated (Fig. 2B, N3H+N5B-J6 and N3H+N5BX-J6).

Then, we tested the infectivity of the culture medium from the RNA-transfected cells by a focus formation assay. The infectivity of the culture medium from JFH-1 RNA-transfected cells was determined as $8.8 \times 10^3 \pm 5.7 \times 10^2$ FFU/ml (Table 1). The infectivity of the culture medium was also detected from cells transfected with J6/N3H+N5BX/JFH-1, JFH-1/N3H-J6, JFH-1/N5B-J6, or JFH-1/3'UTR-J6 RNA but not with other chimeric RNAs (Table 1). This result thus indicates that efficient core protein secretion is at least indispensable for infectious-virus secretion. However, the levels of infectivity of culture medium did not correlate with core protein concentrations. In particular, JFH-1/N3H-J6 RNA-transfected cells secreted a rather higher level of core protein, but its infectious titer was low. The RNA replication capacity of JFH-1/N3H-J6 was lower than that of wild-type JFH-1 or JFH-1/3'UTR-J6

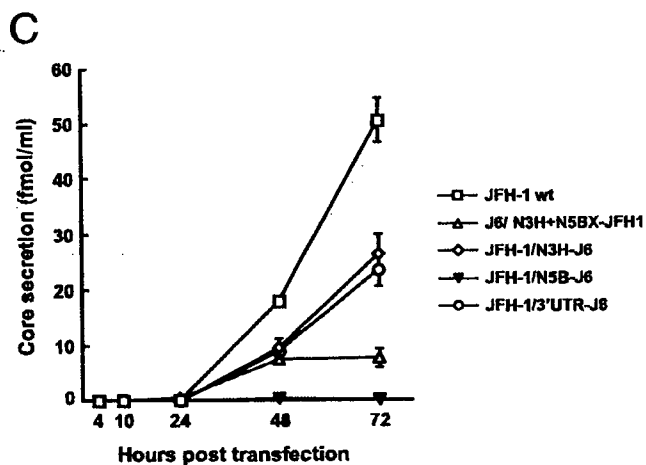
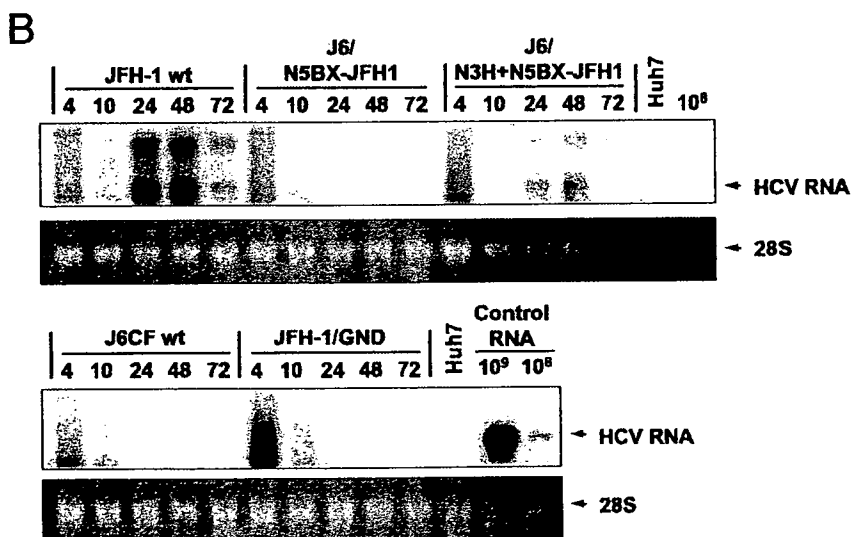
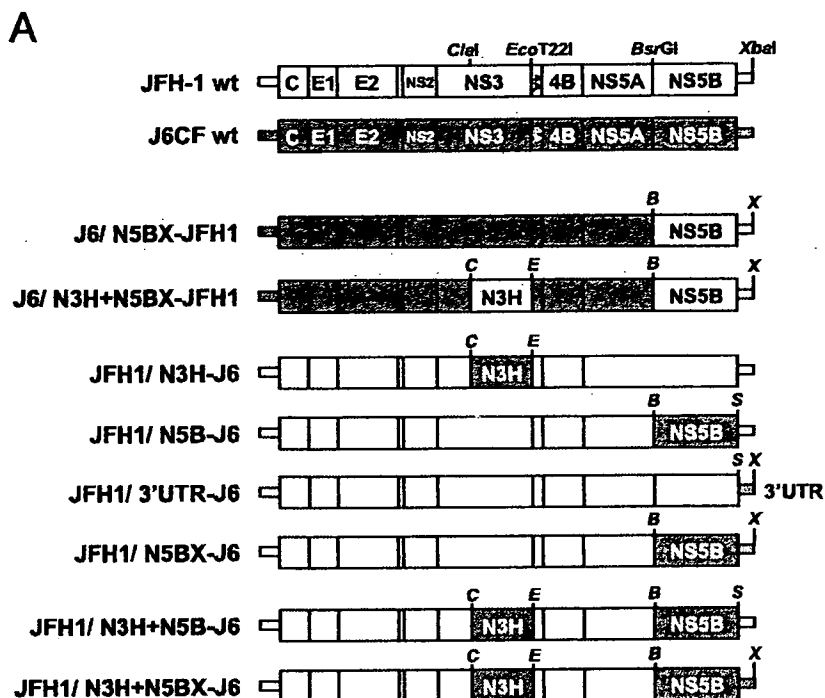


TABLE 1. Infectious titers of the media from chimeric HCV RNA-transfected cells

Construct ^a	Core protein level (fmol/ml)	Infectivity (FFU/ml)
JFH-1 (wild type)	50.7 ± 4.1	8.8 × 10 ³ ± 5.7 × 10 ²
JFH-1/GND	0	0
J6CF (wild type)	0	0
J6/N5BX-JFH1	0	0
J6/N3H+N5BX-JFH1	7.7 ± 1.7	9.1 × 10 ¹ ± 4.1 × 10 ¹
JFH-1/N3H-J6	26.3 ± 3.6	1.7 × 10 ¹ ± 1.2 × 10 ¹
JFH-1/N5B-J6	0.1 ± 0.0	6.7 × 10 ⁰ ± 4.1 × 10 ⁰
JFH-1/3'UTR-J6	23.6 ± 2.9	2.6 × 10 ³ ± 7.1 × 10 ²
JFH-1/N5BX-J6	0	0
JFH-1/N3H+N5B-J6	0	0
JFH-1/N3H+N5BX-J6	0	0

^a Culture media were collected from the RNA-transfected cells 72 h after transfection.

(Fig. 2B), and currently, there is no clear explanation for this discrepancy. This will be further examined in a future study.

Importantly, we found that the J6/N3H+N5BX-JFH1 chimera produced infectious virus. These results strongly indicate that the NS3 helicase and NS5B-to-3'X regions of JFH-1 are important for autonomous replication of the replication-incompetent J6CF strain and for secretion of infectious chimeric virus, although the virus secretion efficiency and the infection efficiency of the secreted virus were low.

DISCUSSION

In the present study, we identified the regions that are important for efficient JFH-1 replication in Huh7 cells by using chimeric constructs with other genotype 2a clones. Via transient replication assays of JFH-1 and J6CF chimeras, both the NS3 helicase-coding (N3H) region and the NS5B-to-3'X (N5BX) region of JFH-1 were found to be important for replication (Fig. 2 and 3). This was also confirmed by full-length genomic RNA replication, but the replication level of J6/N3H+N5BX-JFH1 was lower than that of wild-type JFH-1 (Fig. 5B). The N5BX region of JFH-1 was the minimum essential region for subgenomic-replicon replication (Fig. 3B, N5BX-JFH-1), but in full-length RNA replication, the NS3 helicase-coding region of JFH-1 was also necessary (Fig. 5B). This contradiction might be explained by differences in RNA length, because shorter RNAs such as subgenomic replicons are likely to replicate even with a less powerful replication engine. Alternatively, there could be some negative element for replication in the J6CF structural-protein-coding region or some positive element in the *neo* encephalomyocarditis virus

internal ribosome entry site region of the subgenomic replicon. Furthermore, J6 chimeric RNA with the minimum essential regions of JFH-1 (J6/N3H+N5BX-JFH1) caused Huh7 cells to secrete infectious chimeric virus particles. However, the infection efficiency of J6/N3H+N5BX-JFH1 was lower than that of wild-type JFH-1. First, this may be due to the low RNA replication level. With JFH-1 NS3 helicase and N5BX, J6CF was able to replicate, but the replication efficiency was lower than that of JFH-1 (Fig. 5B). Because J6CF replication could occur only with JFH-1 NS3 helicase and N5BX, more *cis*-acting replication elements (CREs) of JFH-1 may be needed for more efficient replication of J6CF. Second, the levels of virus assembly may be low. This chimera had only the NS3 helicase, NS5B, and 3'UTR regions of JFH-1, possibly omitting some regions important for efficient virus particle secretion. Given that the NS2 region of JFH-1 is reportedly important in virus assembly and release (39), the NS2 region may be a possible candidate. JFH-1/N3H-J6 RNA-transfected cells secreted a substantial amount of core protein; however, its infectivity was much lower (Table 1). The JFH-1 N3H region may be important for the infectivity of the secreted virus and/or for virus particle secretion itself. This will be determined in a future study.

Significance of JFH-1 N5BX for replication. We demonstrated the importance of both the NS5B-coding region and the 3'UTR in JFH-1 replication in the present study. There are several reports regarding CREs within the NS5B-coding region and 3'UTR of Con1 (9, 28, 52). The importance of the interaction between CREs in NS5B and the 3'UTR for replication has also been reported for the Con1 strain (9). The nucleotide sequences involved in the kissing-loop interaction were conserved between JFH-1, J6CF, and Con-1. However, mutations in other regions may affect this interaction by disrupting the RNA secondary structures. On the other hand, given that the NS5B-coding region encodes an RNA-dependent RNA polymerase, the enzymatic activities of the polymerase may differ among the tested strains. The sequence similarities of the JFH-1 and J6CF NS5B regions are 92.2% for the nucleotide sequence and 95.1% for the amino acid sequence. Out of 591 amino acids, only 29 amino acids differ, and the GDD motif that is highly conserved among RdRps is conserved. There are many reports regarding the interaction between NS5B and other viral or cellular proteins, and some of the interactions have been reported to play a role in replication (6, 10, 12, 15, 17, 27, 41–43, 45, 46). Furthermore, the importance of the membrane localization of NS5B with respect to replication has also been reported (29, 35). Mutations in J6CF NS5B may affect these roles. It is thus important to examine the RdRp activities of JFH-1 and J6CF NS5B proteins *in vitro*.

FIG. 5. Analysis of transient replication of genomic chimeric HCV RNA. (A) Structures of full-length chimeric HCV RNAs. Each chimeric full-length construct was prepared by the insertion of the restricted fragments as indicated. The restriction enzyme recognition sites used for the plasmid constructions are indicated. C, ClaI; E, EcoT22I; B, BsrGI; S, StuI; X, XbaI; wt, wild type. (B) Northern blot analysis of total RNA prepared from cells transfected with transcribed genomic HCV RNA. Numbers of synthetic JFH-1 RNA (control RNA), RNA isolated from naïve cells (Huh7), and hours after transfection (4, 10, 24, 48, and 72) are indicated. Arrowheads indicate full-length HCV RNA (HCV RNA) and 28S rRNA (28S). A representative autoradiogram (6-h exposure) of three independent experiments is presented. (C) HCV core protein secretion from the RNA-transfected cells. Transcribed wild-type or chimeric full-length HCV RNAs (10 µg) were transfected into Huh7 cells. Culture medium was harvested at 4, 10, 24, 48, and 72 h after transfection. The amounts of core proteins in the harvested culture medium were measured using an HCV core enzyme-linked immunosorbent assay. The assays were performed five times independently, and data are presented as means and standard deviations.

On the other hand, the effect of the 3'UTR is very surprising, especially since the nucleotide sequences of this region are very similar between JFH-1 and J6CF. In this study, the 3'UTR includes four parts: 22 nucleotides at the 3'-end NS5B region (as a result of the cloning strategy), 39 nucleotides of variable region, the poly(U/UC) region, and a 98-nucleotide 3'X region. There are a single synonymous nucleotide mutation in the 3'-end NS5B region and three nucleotide mutations in the variable region. The poly(U/UC) regions are 99 and 132 nucleotides in JFH-1 and J6CF, respectively. There are no mutations in the 3'X region in either strain. It is thus quite interesting to pursue the mechanisms of these mutations in the 3'UTR that affect the HCV RNA replication levels. Further studies are important for precise elucidation of the efficient replication mechanisms of JFH-1.

Significance of the JFH-1 NS3 helicase region for replication. In the present study, we demonstrated the importance of the JFH-1 NS3 helicase region, especially in full-length genomic RNA replication. It has been reported that an active NS3 helicase is required for replication of subgenomic replicons (25). The NS3 helicase domain possesses helicase activity and ATPase activity, and it has been reported that the characters of these enzymes differ among the genotypes and the strains (26). NS3 has also been reported to interact with positive- and negative-strand RNA 3'UTRs (1). One possible model of the role of NS3 in RNA replication is that NS3 helicase unwinds RNA secondary structures and/or a double-stranded RNA intermediate before RNA synthesis by NS5B (37). The sequence similarity of the NS3 helicase regions of JFH-1 and J6CF is rather high, 89.5% for the nucleotide sequence and 93.8% for the amino acid sequence, and out of 487 amino acids, only 30 amino acids differ. These mutations may affect the enzymatic activities of NS3 helicase.

Furthermore, it has been reported that NS3 can stimulate NS5B RdRp activity (38). It has also been reported that the NS3 protease domain and NS5B stimulate NS3 helicase activity (53). Taken together, these findings show that not only the enzymatic activities themselves but also the combination or interaction of the NS3 and NS5B proteins could be important. However, it is still important to examine and compare the NS3 helicase enzymatic activities in vitro of JFH-1 and other HCV strains in a further study.

Replication in vitro and in vivo. We previously reported that JFH-1 RNA could replicate efficiently in Huh7 cells. Cell-cultured JFH-1 virus was also found to be infectious in chimpanzees; however, the virus was cleared immediately after transient viremia (48). In contrast, J6CF does not replicate in Huh7 cells, but it is infectious in chimpanzees (49). J6/JFH-1 chimeric RNA replicated efficiently in Huh7 cells (39) and Huh7-derived cell lines (30), and cell-cultured chimeric J6/JFH-1 virus was infectious in chimpanzees and in chimeric uPA-SCID mice (31). Replication efficiency in vitro may not necessarily correlate with that in vivo. The H77, Con-1, and HCV-N strains were infectious in chimpanzees (3, 5, 23, 50). However, the H77 and Con-1 strains need adaptive mutations for efficient replication in cultured cells (4, 24) and HCV-N replicates relatively efficiently in cultured cells (16). On the other hand, H77-S containing five adaptive mutations can produce infectious virus particles (51), but the Con-1 and HCV-N strains do not produce virus particles (16, 40). It is still unclear

what viral or host factors are important for efficient replication and infectious-virus production in vitro and in vivo. However, understanding HCV replication mechanisms by using cell culture models is still important for elucidation of the HCV life cycle.

Significance of the regions responsible for JFH-1 replication. Using two HCV strains, JFH-1 and J6CF, which are very closely related but have different characteristics, we were able to determine which regions are important for replication in cultured cells. Replication of two other genotype 2a strains, JCH-1 and JCH-4, was also recovered by replacement of the N3H and N5BX regions of JFH-1 at the lower levels compared to replication of the J6 replicon (Fig. 3B and 4). This may be because J6CF is an infectious clone in chimpanzees, but the JCH-1 and JCH-4 strains are clinical isolates from chronic-hepatitis patients (21) and may include critical mutations in other important regions. Furthermore, replication of genotype 1 HCV replicons was not restored by the same procedure as that for genotype 2a replicons (Fig. 4). Functional complementation in the nonstructural region and 3'UTR may be difficult beyond the genotypes.

Obtaining virus particles is an important step in antiviral research. Although infection efficiency is improved in permissive cell lines, most HCV strains still cannot replicate or produce virus particles in cultured cells. Therefore, chimeric virus particles with the JFH-1 replication engine may be suitable substitutes. Furthermore, analyses using chimeric viruses that have structural proteins and other regions from various strains may give us new information regarding strain-specific effects on HCV life cycles. Consequently, applying the findings of the present study to replication-incompetent strains may be useful not only for analyses of virus strain specificity and precise analyses of the HCV life cycle but also for antiviral studies.

In conclusion, we analyzed the mechanism underlying efficient JFH-1 replication by using intragenotypic chimeras of JFH-1 and J6CF and clearly showed the importance of the JFH-1 NS3 helicase region and the NS5B-to-3'X region for efficient replication of HCV genotype 2a strains.

ACKNOWLEDGMENTS

A.M. is supported by the Viral Hepatitis Research Foundation of Japan, and K.M. is supported by the Japan Health Sciences Foundation. This work was partially supported by a grant-in-aid for Scientific Research from the Japan Society for the Promotion of Science, from the Ministry of Health, Labor and Welfare of Japan, and from the Ministry of Education, Culture, Sports, Science and Technology and by the Research on Health Sciences Focusing on Drug Innovation from the Japan Health Sciences Foundation.

The pJ6CF plasmid was kindly provided by Jens Bukh. The pCV-H77c plasmid was kindly provided by Robert H. Purcell. The pFK-I389/neo/NS3-3'/wt plasmid was kindly provided by Ralf Bartenschlager.

REFERENCES

1. Banerjee, R., and A. Dasgupta. 2001. Specific interaction of hepatitis C virus protease/helicase NS3 with the 3'-terminal sequences of viral positive- and negative-strand RNA. *J. Virol.* 75:1708-1721.
2. Bartenschlager, R., and V. Lohmann. 2000. Replication of hepatitis C virus. *J. Gen. Virol.* 81:1631-1648.
3. Beard, M. R., G. Abell, M. Honda, A. Carroll, M. Gartland, B. Clarke, K. Suzuki, R. Lanford, D. V. Sangar, and S. M. Lemon. 1999. An infectious molecular clone of a Japanese genotype 1b hepatitis C virus. *Hepatology* 30:316-324.
4. Blight, K. J., J. A. McKeating, J. Marcotrigiano, and C. M. Rice. 2003.

- Efficient replication of hepatitis C virus genotype 1a RNAs in cell culture. *J. Virol.* 77:3181–3190.
5. Bukh, J., T. Pietschmann, V. Lohmann, N. Krieger, K. Faulk, R. E. Engle, S. Govindarajan, M. Shapiro, M. St. Claire, and R. Bartenschlager. 2002. Mutations that permit efficient replication of hepatitis C virus RNA in Huh-7 cells prevent productive replication in chimpanzees. *Proc. Natl. Acad. Sci. USA* 99:14416–14421.
 6. Choi, S. H., K. J. Park, B. Y. Ahn, G. Jung, M. M. Lai, and S. B. Hwang. 2006. Hepatitis C virus nonstructural 5B protein regulates tumor necrosis factor alpha signaling through effects on cellular I κ B kinase. *Mol. Cell. Biol.* 26:3048–3059.
 7. Choo, Q. L., G. Kuo, A. J. Weiner, L. R. Overby, D. W. Bradley, and M. Houghton. 1989. Isolation of a cDNA clone derived from a blood-borne non-A, non-B viral hepatitis genome. *Science* 244:359–362.
 8. Choo, Q. L., K. H. Richman, J. H. Han, K. Berger, C. Lee, C. Dong, C. Gallegos, D. Coit, R. Medina-Selby, P. J. Barr, et al. 1991. Genetic organization and diversity of the hepatitis C virus. *Proc. Natl. Acad. Sci. USA* 88:2451–2455.
 9. Friebe, P., J. Boudet, J. P. Simorre, and R. Bartenschlager. 2005. Kissing-loop interaction in the 3' end of the hepatitis C virus genome essential for RNA replication. *J. Virol.* 79:380–392.
 10. Gao, L., H. Tu, S. T. Shi, K. J. Lee, M. Asanaka, S. B. Hwang, and M. M. Lai. 2003. Interaction with a ubiquitin-like protein enhances the ubiquitination and degradation of hepatitis C virus RNA-dependent RNA polymerase. *J. Virol.* 77:4149–4159.
 11. Grakoui, A., C. Wychowski, C. Lin, S. M. Feinstone, and C. M. Rice. 1993. Expression and identification of hepatitis C virus polyprotein cleavage products. *J. Virol.* 67:1385–1395.
 12. Hamamoto, I., Y. Nishimura, T. Okamoto, H. Aizaki, M. Liu, Y. Mori, T. Abe, T. Suzuki, M. M. Lai, T. Miyamura, K. Moriishi, and Y. Matsuura. 2005. Human VAP-B is involved in hepatitis C virus replication through interaction with NSSA and NSSB. *J. Virol.* 79:13473–13482.
 13. Hijikata, M., N. Kato, Y. Ootsuyama, M. Nakagawa, and K. Shimotohno. 1991. Gene mapping of the putative structural region of the hepatitis C virus genome by in vitro processing analysis. *Proc. Natl. Acad. Sci. USA* 88:5547–5551.
 14. Hijikata, M., H. Mizushima, Y. Tanji, Y. Komoda, Y. Hirowatari, T. Akagi, N. Kato, K. Kimura, and K. Shimotohno. 1993. Proteolytic processing and membrane association of putative nonstructural proteins of hepatitis C virus. *Proc. Natl. Acad. Sci. USA* 90:10773–10777.
 15. Hirano, M., S. Kaneko, T. Yamashita, H. Luo, W. Qin, Y. Shirota, T. Nomura, K. Kobayashi, and S. Murakami. 2003. Direct interaction between nucleolin and hepatitis C virus NS5B. *J. Biol. Chem.* 278:5109–5115.
 16. Ikeda, M., M. Yi, K. Li, and S. M. Lemon. 2002. Selectable subgenomic and genome-length dicistronic RNAs derived from an infectious molecular clone of the HCV-N strain of hepatitis C virus replicate efficiently in cultured Huh7 cells. *J. Virol.* 76:2997–3006.
 17. Ishido, S., T. Fujita, and H. Hotta. 1998. Complex formation of NS5B with NS3 and NS4A proteins of hepatitis C virus. *Biochem. Biophys. Res. Commun.* 244:35–40.
 18. Kato, N., M. Hijikata, Y. Ootsuyama, M. Nakagawa, S. Ohkoshi, T. Sugimura, and K. Shimotohno. 1990. Molecular cloning of the human hepatitis C virus genome from Japanese patients with non-A, non-B hepatitis. *Proc. Natl. Acad. Sci. USA* 87:9524–9528.
 19. Kato, T., T. Date, M. Miyamoto, A. Furusaka, K. Tokushige, M. Mizokami, and T. Wakita. 2003. Efficient replication of the genotype 2a hepatitis C virus subgenomic replicon. *Gastroenterology* 125:1808–1817.
 20. Kato, T., T. Date, M. Miyamoto, M. Sugiyama, Y. Tanaka, E. Orito, T. Ohno, K. Sugihara, I. Hasegawa, K. Fujiwara, K. Ito, A. Ozasa, M. Mizokami, and T. Wakita. 2005. Detection of anti-hepatitis C virus effects of interferon and ribavirin by a sensitive replicon system. *J. Clin. Microbiol.* 43:5679–5684.
 21. Kato, T., A. Furusaka, M. Miyamoto, T. Date, K. Yasui, J. Hiramoto, K. Nagayama, T. Tanaka, and T. Wakita. 2001. Sequence analysis of hepatitis C virus isolated from a fulminant hepatitis patient. *J. Med. Virol.* 64:334–339.
 22. Kiyosawa, K., T. Sodeyama, E. Tanaka, Y. Gibo, K. Yoshizawa, Y. Nakano, S. Furuta, Y. Akahane, K. Nishioka, R. H. Purcell, et al. 1990. Interrelationship of blood transfusion, non-A, non-B hepatitis and hepatocellular carcinoma: analysis by detection of antibody to hepatitis C virus. *Hepatology* 12:671–675.
 23. Kolykhalov, A. A., E. V. Agapov, K. J. Blight, K. Mihalik, S. M. Feinstone, and C. M. Rice. 1997. Transmission of hepatitis C by intrahepatic inoculation with transcribed RNA. *Science* 277:570–574.
 24. Krieger, N., V. Lohmann, and R. Bartenschlager. 2001. Enhancement of hepatitis C virus RNA replication by cell culture-adaptive mutations. *J. Virol.* 75:4614–4624.
 25. Lam, A. M., and D. N. Frick. 2006. Hepatitis C virus subgenomic replicon requires an active NS3 RNA helicase. *J. Virol.* 80:404–411.
 26. Lam, A. M., D. Keeney, P. Q. Eckert, and D. N. Frick. 2003. Hepatitis C virus NS3 ATPases/helicases from different genotypes exhibit variations in enzymatic properties. *J. Virol.* 77:3950–3961.
 27. Lan, S., H. Wang, H. Jiang, H. Mao, X. Liu, X. Zhang, Y. Hu, L. Xiang, and Z. Yuan. 2003. Direct interaction between alpha-actinin and hepatitis C virus NSSB. *FEBS Lett.* 554:289–294.
 28. Lee, H., H. Shin, E. Wimmer, and A. V. Paul. 2004. cis-Acting RNA signals in the NSSB C-terminal coding sequence of the hepatitis C virus genome. *J. Virol.* 78:10865–10877.
 29. Lee, K. J., J. Choi, J. H. Ou, and M. M. Lai. 2004. The C-terminal transmembrane domain of hepatitis C virus (HCV) RNA polymerase is essential for HCV replication in vivo. *J. Virol.* 78:3797–3802.
 30. Lindenbach, B. D., M. J. Evans, A. J. Syder, B. Wolk, T. L. Tellinghuisen, C. C. Liu, T. Maruyama, R. O. Hynes, D. R. Burton, J. A. McKeating, and C. M. Rice. 2005. Complete replication of hepatitis C virus in cell culture. *Science* 309:623–626.
 31. Lindenbach, B. D., P. Meuleman, A. Ploss, T. Vanwolleghem, A. J. Syder, J. A. McKeating, R. E. Lanford, S. M. Feinstone, M. E. Major, G. Leroux-Roels, and C. M. Rice. 2006. Cell culture-grown hepatitis C virus is infectious in vivo and can be recultured in vitro. *Proc. Natl. Acad. Sci. USA* 103:3805–3809.
 32. Lohmann, V., F. Korner, J. Koch, U. Herian, L. Theilmann, and R. Bartenschlager. 1999. Replication of subgenomic hepatitis C virus RNAs in a hepatoma cell line. *Science* 285:110–113.
 33. McLauchlan, J., M. K. Lemberg, G. Hope, and B. Martoglio. 2002. Intramembrane proteolysis promotes trafficking of hepatitis C virus core protein to lipid droplets. *EMBO J.* 21:3980–3988.
 34. Miyamoto, M., T. Kato, T. Date, M. Mizokami, and T. Wakita. 2006. Comparison between subgenomic replicons of hepatitis C virus genotypes 2a (JFH-1) and 1b (Con1 NK5.1). *Intervirology* 49:37–43.
 35. Moradpour, D., V. Brass, E. Bieck, P. Friebe, R. Gosert, H. E. Blum, R. Bartenschlager, F. Penin, and V. Lohmann. 2004. Membrane association of the RNA-dependent RNA polymerase is essential for hepatitis C virus RNA replication. *J. Virol.* 78:13278–13284.
 36. Nakabayashi, H., K. Taketa, K. Miyano, T. Yamane, and J. Sato. 1982. Growth of human hepatoma cells lines with differentiated functions in chemically defined medium. *Cancer Res.* 42:3858–3863.
 37. Paolini, C., R. De Francesco, and P. Gallinari. 2000. Enzymatic properties of hepatitis C virus NS3-associated helicase. *J. Gen. Virol.* 81:1335–1345.
 38. Piccininni, S., A. Varaklioti, M. Nardelli, B. Dave, K. D. Raney, and J. E. McCarthy. 2002. Modulation of the hepatitis C virus RNA-dependent RNA polymerase activity by the non-structural (NS) 3 helicase and the NS4B membrane protein. *J. Biol. Chem.* 277:45670–45679.
 39. Pietschmann, T., A. Kaul, G. Koutsoudakis, A. Shavinskaya, S. Kallis, E. Steinmann, K. Abid, F. Negro, M. Dreux, F. L. Cosset, and R. Bartenschlager. 2006. Construction and characterization of infectious intragenotypic and intergenotypic hepatitis C virus chimeras. *Proc. Natl. Acad. Sci. USA* 103:7408–7413.
 40. Pietschmann, T., V. Lohmann, A. Kaul, N. Krieger, G. Rinck, G. Rutter, D. Strand, and R. Bartenschlager. 2002. Persistent and transient replication of full-length hepatitis C virus genomes in cell culture. *J. Virol.* 76:4008–4021.
 41. Shimakami, T., M. Hijikata, H. Luo, Y. Y. Ma, S. Kaneko, K. Shimotohno, and S. Murakami. 2004. Effect of interaction between hepatitis C virus NSSA and NSSB on hepatitis C virus RNA replication with the hepatitis C virus replicon. *J. Virol.* 78:2738–2748.
 42. Shimakami, T., M. Honda, T. Kusakawa, T. Murata, K. Shimotohno, S. Kaneko, and S. Murakami. 2006. Effect of hepatitis C virus (HCV) NS5B-nucleolin interaction on HCV replication with HCV subgenomic replicon. *J. Virol.* 80:3332–3340.
 43. Shirota, Y., H. Luo, W. Qin, S. Kaneko, T. Yamashita, K. Kobayashi, and S. Murakami. 2002. Hepatitis C virus (HCV) NSSA binds RNA-dependent RNA polymerase (RdRP) NS5B and modulates RNA-dependent RNA polymerase activity. *J. Biol. Chem.* 277:11149–11155.
 44. Takamizawa, A., C. Mori, I. Fuke, S. Manabe, S. Murakami, J. Fujita, E. Onishi, T. Andoh, I. Yoshida, and H. Okayama. 1991. Structure and organization of the hepatitis C virus genome isolated from human carriers. *J. Virol.* 65:1105–1113.
 45. Tu, H., L. Gao, S. T. Shi, D. R. Taylor, T. Yang, A. K. Mircheff, Y. Wen, A. E. Gorbalenya, S. B. Hwang, and M. M. Lai. 1999. Hepatitis C virus RNA polymerase and NS5A complex with a SNARE-like protein. *Virology* 263:30–41.
 46. Uchida, M., N. Hino, T. Yamanaka, H. Fukushima, T. Imanishi, Y. Uchiyama, T. Kodama, and T. Doi. 2002. Hepatitis C virus core protein binds to a C-terminal region of NS5B RNA polymerase. *Hepatol. Res.* 22:297–306.
 47. van den Hoff, M. J., A. F. Moorman, and W. H. Lamers. 1992. Electroporation in 'intracellular' buffer increases cell survival. *Nucleic Acids Res.* 20:2902.
 48. Wakita, T., T. Pietschmann, T. Kato, T. Date, M. Miyamoto, Z. Zhao, K. Murthy, A. Habermann, H. G. Krausslich, M. Mizokami, R. Bartenschlager, and T. J. Liang. 2005. Production of infectious hepatitis C virus in tissue culture from a cloned viral genome. *Nat. Med.* 11:791–796.
 49. Yanagi, M., R. H. Purcell, S. U. Emerson, and J. Bukh. 1999. Hepatitis C virus: an infectious molecular clone of a second major genotype (2a) and lack of viability of intertypic 1a and 2a chimeras. *Virology* 262:250–263.
 50. Yanagi, M., R. H. Purcell, S. U. Emerson, and J. Bukh. 1997. Transcripts

- from a single full-length cDNA clone of hepatitis C virus are infectious when directly transfected into the liver of a chimpanzee. *Proc. Natl. Acad. Sci. USA* **94**:8738–8743.
51. Yi, M., R. A. Villanueva, D. L. Thomas, T. Wakita, and S. M. Lemon. 2006. Production of infectious genotype 1a hepatitis C virus (Hutchinson strain) in cultured human hepatoma cells. *Proc. Natl. Acad. Sci. USA* **103**:2310–2315.
52. You, S., D. D. Stump, A. D. Branch, and C. M. Rice. 2004. A *cis*-acting replication element in the sequence encoding the NS5B RNA-dependent RNA polymerase is required for hepatitis C virus RNA replication. *J. Virol.* **78**:1352–1366.
53. Zhang, C., Z. Cai, Y. C. Kim, R. Kumar, F. Yuan, P. Y. Shi, C. Kao, and G. Luo. 2005. Stimulation of hepatitis C virus (HCV) nonstructural protein 3 (NS3) helicase activity by the NS3 protease domain and by HCV RNA-dependent RNA polymerase. *J. Virol.* **79**:8687–8697.
54. Zhong, J., P. Gastaminza, G. Cheng, S. Kapadia, T. Kato, D. R. Burton, S. F. Wieland, S. L. Uprichard, T. Wakita, and F. V. Chisari. 2005. Robust hepatitis C virus infection in vitro. *Proc. Natl. Acad. Sci. USA* **102**:9294–9299.

Original Article

An infectious and selectable full-length replicon system with hepatitis C virus JFH-1 strain

Tomoko Date,^{1*} Michiko Miyamoto,¹ Takanobu Kato,^{2,3} Kenichi Morikawa,^{1*} Asako Murayama,^{1*} Daisuke Akazawa,^{1,4*} Junichi Tanabe,^{1,4} Saburo Sone,⁴ Masashi Mizokami² and Takaji Wakita^{1*}

¹Department of Microbiology, Tokyo Metropolitan Institute for Neuroscience, Tokyo, ²Department of Clinical Molecular Informative Medicine, Nagoya City University Graduate School of Medical Sciences, Nagoya, and ⁴Pharmaceutical Research Laboratory, Toray Industries Inc., Kanagawa, Japan; and ³Liver Disease Branch, NIDDK, National Institute of Health, Bethesda, Maryland, USA

Aim: The hepatitis C virus (HCV) strain JFH-1 was cloned from a patient with fulminant hepatitis. A JFH-1 subgenomic replicon and full-length JFH-1 RNA efficiently replicate in cultured cells. In this study, an infectious, selectable HCV replicon containing full-length JFH-1 cDNA was constructed.

Methods: The full-genome replicon was constructed using the neomycin-resistant gene, EMCV IRES and wild-type JFH-1 cDNA. Huh7 cells were transfected with RNA synthesized *in vitro*, and then cultured with G418. Independent colonies were cloned to establish cell lines that replicate the full-length HCV replicon.

Results: HCV RNA replication was detected in each isolated cell line. HCV proteins and HCV RNA were secreted into

culture medium, and exhibited identical density profiles. Interestingly, culture supernatants of the replicon cells were infectious for naïve Huh7 cells. Long-term culture did not affect replication of replicon RNA in the replicon cells, but it reduced core protein secretion and infectivity of culture supernatant. Culture supernatant obtained after serial passage of replicon virus was infectious for Huh7 cells.

Conclusions: Selectable infection was established using HCV replicon containing full-length genotype 2a JFH-1 cDNA. This system might be useful for HCV research.

Key words: hepatitis C virus, infectious virus, replicon, RNA replication

INTRODUCTION

HEPATITIS C VIRUS (HCV) is a plus-strand RNA virus and is the principal cause of post-transfusion hepatitis and sporadic acute hepatitis.^{1,2} Infection with HCV causes chronic liver diseases, including cirrhosis and hepatocellular carcinoma.³ Although HCV belongs to the *Flaviviridae* family, and has a genome structure similar to other flaviviruses, it has been difficult to develop an efficient cell culture system for HCV.⁴ A subgenomic HCV RNA replicon system has been developed,⁵ enabling assessment of HCV replication in cultured cells. Although that system is a powerful tool for

studies of HCV replication mechanisms and development of antiviral agents, its replicon cells do not produce infectious viral particles, even when the replicons contain structural genes.^{6,7} Studies conducted using the above replicon system indicate that wild-type HCV genomes have low replication capacities.^{7,8}

Adaptive mutations can substantially increase replication of HCV, but introduction of these adaptive mutations into full-length genomes causes loss of infectivity *in vivo*.⁸ The JFH-1 strain was cloned from a patient with fulminant hepatitis, and its sequence differs from those of chronic hepatitis isolates.⁹ Using JFH-1 cDNA, we previously established subgenomic replicon constructs that replicate in Huh7 cells with greater efficiency than other HCV strains, and that also replicate in other cell lines.^{10,11} In a previous study, when we transfected Huh7 cells with *in-vitro*-transcribed full-length JFH-1 HCV RNA, the JFH-1 RNA efficiently replicated and the cells produced viral particles that were infectious for cultured cells and a chimpanzee.¹² In the present study, we established a full-length HCV replicon using the JFH-1 strain.

Correspondence: Dr Takaji Wakita, Department of Virology II, National Institute of Infectious Diseases, 1-23-1 Toyama, Shinjuku, Tokyo 162-8640, Japan. Email: wakita@nih.go.jp

*Present address: Department of Virology II, National Institute of Infectious Diseases, Tokyo, Japan.

Received 10 November 2006; revision 4 December 2006; accepted 5 December 2006.

Replicon virus particles were secreted from the replicon cells, and the replicon virus was infectious for naïve Huh7 cells.

METHODS

Cell culture system

HUH7 CELLS WERE donated by Dr Tetsuro Suzuki (National Institute of Infectious Diseases, Tokyo, Japan), and were cultured at 37°C in Dulbecco's modified Eagle's medium containing 10% fetal bovine serum (DMEM-10), as previously described.¹⁰

Construction of the full-genome HCV replicon

A full-genome replicon construct of JFH-1 (pFGR-JFH1; Fig. 1a) was assembled based on the consensus sequence of JFH-1, as follows. The gene for the encephalomyocarditis virus (EMCV) internal ribosomal entry site (IRES) was amplified from a subgenomic replicon construct of JFH-1 (pSGR-JFH1; Fig. 1a)¹⁰ using

the primers Pm/EI-S (5'-AGC TTT GTT TAA ACC CTC TCC CTC CCC CCC CCC TAA CGT T-3'; the underlined segment is the *PmeI* site) and EI/FH/Core-R (5'-TGA GGT TTA GGA TTT GTG CTC ATG GTA TCA TCG TGT TTT T-3'). The core region was amplified from pJFH1¹² using the primers EI/FH/Core-S (5'- TTC AAA AAC ACC ATG ATA CCA TGA GCA CAA ATC CTA AAC C-3') and FH/1592-R (5'- CGG TTG ATG TGC CAA CTG CC-3'). These two polymerase chain reaction (PCR) fragments were purified, mixed and reamplified using the primers Pm/EI-S and FH/1592-R. Reamplified PCR product was digested with *PmeI* and *BsiWI*. Another DNA fragment containing a 5' untranslated region (5' UTR) and neomycin-resistant gene was digested from pSGR-JFH1 using *AgeI* and *PmeI* (Fig. 1a). These two DNA fragments were cloned into the vector pJFH1 at sites for *AgeI* and *BsiWI* to produce the pFGR-JFH1 construct (accession number: AB237837, Fig. 1a).

As a control, we also created the mutant construct pFGR-JFH1/GND that includes a point mutation that changes a GDD motif to GND, which abolishes the RNA polymerase activity of non-structural protein (NS) 5B.¹⁰

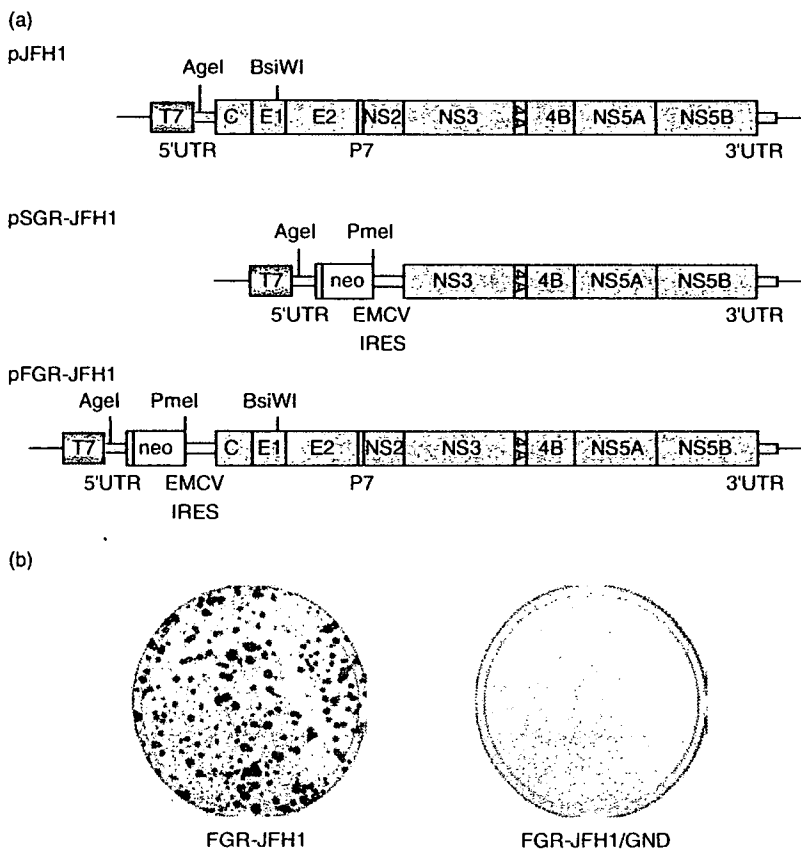


Figure 1 Structure of the full-genome hepatitis C virus (HCV) RNA replicon constructed from genotype 2a JFH-1 and colony formation of replicon RNA-transfected Huh7 cells. (a) Organization of the full-length JFH-1 genome (top), subgenomic replicon construct pSGR-JFH1 (middle) and full-genome replicon construct pFGR-JFH1 (bottom). Open reading frames (thick boxes) are flanked by untranslated regions (thin boxes). 'Agel', 'BsiWI' and 'PmeI' indicate positions of restriction sites. A T7 RNA promoter is located upstream from the 5' end of the replicon construct. (b) Colony formation of JFH-1 HCV full-genome replicon. Huh7 cells were transfected with transcribed RNA (1 µg), and transfected cells were cultured in medium supplemented with G418 (1 mg/mL) for 3 weeks before staining with crystal violet.

All plasmid DNA was transformed using DH5 α -competent cells. Amplified plasmid DNA was purified by performing ultra-centrifugation twice.

RNA synthesis

Replicon RNA was synthesized as described previously.^{10,12} Briefly, the plasmid pFGR-JFH1 was digested with *Xba*I and treated with Mung Bean nuclease (New England Biolabs, Beverly, MA, USA). Digested plasmid DNA fragments were purified and used as templates for RNA synthesis. HCV RNA was synthesized *in vitro* using a MEGAscript T7 kit (Ambion, Austin, TX, USA). Synthesized RNA was treated with DNaseI, followed by acid phenol extraction to remove any remaining template DNA.

RNA transfection and colony formation experiment

Synthesized replicon RNA was used for transfection via electroporation. Synthesized RNA (0.1 ng to 10 μ g) was adjusted to 10 μ g with cellular RNA isolated from untransfected Huh7 cells. Naïve Huh7 cells were transfected with transcribed replicon RNA from pFGR-JFH1, or were transfected with control RNA transcribed from pFGR-JFH1/GND, in which the catalytic domain of the RNA polymerase NS5B is mutated. Trypsinized Huh7 cells were washed with Opti-MEM I reduced-serum medium (Invitrogen, Carlsbad, CA, USA) and resuspended at 7.5×10^6 cells/mL with Cytomix buffer.¹⁰ RNA (10 μ g) was mixed with 400 μ L of cell suspension and transferred to an electroporation cuvette (Precision Universal Cuvettes, Thermo Hybrid, Middlesex, UK). The cells were then pulsed at 260 V and 950 μ F with the Gene Pulser II apparatus (Bio-Rad, Hercules, CA, USA). Transfected cells were immediately transferred to 10-cm culture dishes, each containing 8 mL of culture medium. G418 (1.0 mg/mL) (Nacalai Tesque, Kyoto, Japan) was added to the culture medium at 16–24 h after transfection. Culture medium supplemented with G418 was replaced twice per week.

Three weeks after transfection, cells were fixed with buffered formalin and stained with crystal violet. Colony formation efficiency of the transfected cells was determined by counting the number of colonies that formed.

Analysis of G418-resistant cells

Sparsely grown G418-resistant colonies were independently isolated using a cloning cylinder (Asahi Techno Glass, Tokyo, Japan), and were expanded until they were 80–90% confluent in 10-cm dishes. Expanded cells were

harvested for nucleic acid and protein analyses. Total RNA and genomic DNA were simultaneously isolated from expanded cells using the Isogen reagent (Nippon Gene, Tokyo, Japan). Another portion of each cell pellet was dissolved with radioimmune precipitation assay (RIPA) buffer containing 0.1% SDS. Eight cloned cell lines were selected for further analysis.

Northern blot analysis

Isolated RNA fragments (4 μ g) were separated in a 1% agarose gel containing formaldehyde, transferred to a positively charged nylon membrane (Hybond-N+, Amersham Pharmacia, Buckinghamshire, UK), and immobilized by Stratalinker UV crosslinker (Stratagene, La Jolla, CA, USA). Replicon RNA was detected using probes specific for certain positions. Hybridization was performed using a [α -³²P]dCTP-labeled DNA probe and Rapid-Hyb buffer (Amersham Pharmacia). The DNA probe was synthesized from the genes *neo'* and EMCV IRES, using the Megaprime DNA labeling system (Amersham Pharmacia).

Western blotting and immunofluorescence analysis

We analyzed protein expression in replicon cells by performing western blotting and immunofluorescence. Cells were lysed using a RIPA buffer containing 0.1% SDS, 0.5% NP-40, 10 mM Tris-HCl (pH 7.4), 1 mM ethylenediaminetetraacetic acid (EDTA), and 150 mM NaCl. Protein samples were separated on 10% or 12% polyacrylamide gels, and were subsequently transferred to a polyvinylidene difluoride membrane (Millipore, Tokyo, Japan). Transferred proteins were incubated with blocking buffer containing 5% non-fat dried milk in phosphate-buffered saline (PBS). HCV proteins were detected using anticore monoclonal antibodies (25, clone 2H9), anti-E1 and anti-E2 polyclonal antibodies,¹² anti-NS3 polyclonal antibodies,¹⁰ anti-NS5A polyclonal antibodies,¹¹ peroxidase-labeled goat antirabbit IgG (Biosource), and peroxidase-labeled sheep antimouse IgG (Amersham Pharmacia). Signals were detected using a chemiluminescence system (Amersham Pharmacia).

Cells containing the HCV replicon were grown on a cover glass, and were then fixed in acetone-methanol (1:1 v/v) for 10 min at -20°C . Cells were then incubated in immunofluorescence assay buffer (PBS, 1% bovine serum albumin, 2.5 mM EDTA). Anti-core monoclonal antibodies or anti-NS3 and anti-NS5a polyclonal antibodies were added at 50 μ g/mL or a dilution of 1:50, respectively, in immunofluorescence buffer. After incubation for 1 h at room temperature, cells were washed,

followed by incubation with fluorescein isothiocyanate-conjugated antimouse IgG (Cappel, Durham, NC, USA) in immunofluorescence assay buffer. Cover slips were washed and mounted on glass slides using Shandon PermaFluor mounting solution (Thermo Electron, Pittsburgh, PA, USA). Cells were examined by fluorescence microscopy (Carl Zeiss, Oberkochen, Germany).

To assay secretion of viral protein and virus particles into culture medium from cells replicating replicon RNA, we measured levels of core protein in culture medium using a sensitive immunoassay. Culture supernatants from all eight replicon cell lines were used in this immunoassay.

Genomic DNA PCR

To detect integration of the *neo'* gene into the genomic DNA, isolated cellular genomic DNA was amplified by PCR using *neo'*-specific primers (NEO-S3; 5'-AACAA GATGGATTGCACGCA-3', NEO-R; 5'-CGTCAAGAAG GCCATAGAAG-3').

RT-PCR and sequencing analysis

We sequenced the replicating HCV RNA in each of the eight selected clones. The cDNAs of the HCV RNA replicon were synthesized from total RNA isolated from cells using a reverse primer for the 3'× region. These cDNAs were subsequently amplified with DNA polymerase (TaKaRa LA *Taq*, Takara Bio, Shiga, Japan). Six separate PCR primer sets were used to amplify the following sections of the pFGR-JFH1 replicon construct, to cover the entire open reading frame: nt 151–2043, nt 1913–3778, nt 3597–6046, nt 5997–8685, nt 8649–10782, and nt 10713–11017. The sequence of each amplified DNA was determined.

Quantification of HCV core protein and RNA

To estimate levels of HCV core protein in culture supernatant, concentrations of HCV core protein were measured. Aliquots (250 µL) of samples were assayed using a new immunoassay technique described elsewhere.¹³ Total RNA was isolated from harvested cells or culture media using Isogen. Copy numbers of HCV RNA were determined by real-time detection reverse transcription (RT)-PCR, using an ABI Prism 7700 sequence detector system (Applied Biosystems, Tokyo, Japan).¹⁴

Density gradient analysis

To determine whether secreted viral core protein was incorporated in viral particles, we analyzed culture medium by sucrose density gradient centrifugation. Culture medium derived from replicon cells was

harvested for density gradient analysis. Collected culture medium was cleared by low-speed centrifugation at 2000 r.p.m. for 10 min, and was then passed through a disk filter with a pore size of 0.45 µm (Millipore). Filtered culture medium was layered on a stepwise sucrose gradient (60% to 10%, wt/vol) and centrifuged for 16 h in a SW41 rotor (Beckman, Palo Alto, CA, USA) at 40 000 r.p.m. at 4°C. After centrifugation, 22 fractions were harvested from the bottoms of the tubes. The core protein concentration of each fraction was measured by performing an immunoassay using 100 µL of the fraction. The HCV RNA titer of each fraction was determined by real time detection RT-PCR using RNA isolated from 100 µL of the fraction.

Infectivity of secreted viral particles

To assess the infectivity of secreted viral particles, naïve Huh7 cells were inoculated with culture supernatant from replicon cell lines. Culture supernatant used for inoculation was centrifuged and filtered to remove cell debris. Cleared culture supernatant was concentrated by ultrafiltration as described previously,¹² and G418 was removed from the concentrated culture supernatant during ultrafiltration. Naïve Huh7 cells were inoculated with concentrated culture medium. Inoculated cells were cultured for 3 weeks in medium supplemented with G418 (0.3 mg/mL).

Long-term culture of replicon cells

To examine replicon RNA replication and virus secretion and infectivity after long-term culture, the eight replicon clones were serially passaged for more than 7 months. HCV RNA levels in replicon cells were measured by real time detection RT-PCR. Infectivity of culture supernatants was determined by measuring colony formation efficiency.

Serial passage of replicon virus

To examine long-term replicon virus passage, replicon virus was serially passaged for approximately 6 months. Culture supernatants harvested from the replicon-RNA-transfected Huh7 cells were used to inoculate naïve Huh7 cells. Inoculated cells formed colonies after 4 weeks of G418 selection culture. This infection and selection procedure was repeated seven times. Infectivity of culture supernatants was determined by measuring colony formation.

Statistical analysis

Statistical analysis was performed using the Mann-Whitney *U*-test or Student's *t*-test. *P*-values of <0.05 were considered to indicate significance.

RESULTS

Construction of full-genome replicon using JFH-1, and colony formation

FIGURE 1A SHOWS the full-genome replicon construct pFGR-JFH1, which was produced from the full-length JFH-1 construct pJFH1 and which contains a neomycin-resistant gene.¹² Huh7 cells transfected with pFGR-JFH1 replicon RNA formed colonies efficiently (Fig. 1b). Huh7 cells transfected with control RNA transcribed from pFGR-JFH1/GND did not form colonies. Cells transfected with full-genome replicon RNA formed colonies 80.7-fold less efficiently than cells transfected with JFH-1 subgenomic replicon RNA (Table 1).¹⁰

Analysis of replicon cells

Figure 2a shows the results of northern blot analysis of replicon RNA replication in the cloned cell lines using cellular RNA extracted from each replicon cell. Intensities of replicon RNA signals differed among the eight clones. Replicon RNAs were clearly identified at the same position as in control RNA; however, additional specific signals were present higher on the gel as was also observed in subgenomic replicon cells.¹⁰ These signals may represent replication intermediates or double-stranded RNA. The replicon RNA titer ranged from 1.14×10^7 to 7.09×10^7 copies/ μg cellular RNA (Table 2). We also estimated the replicon RNA copy numbers per cell. Full-genome replicon cell clones were harvested and counted 2 days after passage. Mean HCV RNA titer of eight full-genomic replicon clones was 6.93×10^3 copy/cell. RNA replication levels in the full-genomic replicon cells were at the similar level with subgenomic JFH-1 replicon cells.¹⁰

Figure 2b shows the results of western blot analysis. In the cell lysate extracted from each replicon cell, we detected core, E1, E2, NS3 and NS5a proteins at the expected positions. Signals detected by anti-NS5a antibody exhibited doublet bands that may represent p58 and p56 with different degrees of phosphorylation.

Figure 2c shows the results of the immunofluorescence assay. In replicon clone 3 (Fig. 2c) and other clones (data not shown), core protein exhibited a

perinuclear punctuate staining pattern, and NS3 and NS5a proteins exhibited a cytoplasmic diffuse staining pattern.

Table 2 shows the results of the immunoassay of core protein in culture medium. Figure 3a shows the results of sucrose density gradient centrifugation of the culture medium of clone 3. Core protein and HCV RNA exhibited identical peaks in a single fraction with a density of approximately 1.16 g/mL (Fig. 3a); this density is similar to that of wild-type JFH-1 virus particles.¹² This result indicates that viral particles were secreted from cells that replicated replicon RNA.

Cells inoculated with culture supernatant of full-genome replicon cell lines formed visible colonies by G418 (1 mg/mL) selection culture for 10–14 days after inoculation; these cells were fixed and stained. In the preliminary experiment, very few colonies formed (data not shown). Consequently, to increase colony formation efficiency after inoculation, the inoculated Huh7 cells were passed 1 day before seeding, culture supernatants from replicon cell lines were concentrated by ultrafiltration as described previously,¹² and inoculated cells were cultured with a lower concentration of G418 (0.3 mg/mL). These changes increased the number of colonies that formed, and colony formation by cells inoculated with supernatant of full-genome replicon cell lines occurred in a dose-dependent manner (Fig. 3b, FGR-JFH1). No colonies were formed by cells inoculated with culture supernatant of subgenomic replicon cells (Fig. 3b, SGR-JFH1).

When genomic DNA from each clone was isolated and amplified by PCR using *neo^r*-specific primers, we did not detect any signals (data not shown).

Long-term culture of replicon cells

Figure 4 shows the results of serial passaging of clones 3 and 5. Core protein titer of culture supernatant of clone 3 decreased rapidly at 50 days of culture. In contrast, core protein titer of culture medium of clone 5 gradually decreased throughout the observation period (Fig. 4a). HCV RNA replication levels in the cells ranged from 1.6×10^7 to 7.8×10^7 copies/ μg RNA, with no significant differences between clones (Fig. 4a). Colony formation efficiency of clone 3 decreased significantly at 50 days of culture (Fig. 4b). Colony formation efficiency of clone 5 decreased gradually throughout the observation period (Fig. 4b).

Serial passages of replicon virus

The HCV RNA levels in the inoculated cells did not change significantly during the observation period

Table 1 Colony formation efficiency of JFH-1 replicon

Replicon	JFH-1 (c.f.u./ μg RNA)
Subgenomic	$5.32 \times 10^4 \pm 5.02 \times 10^4$ †
Full-genome	$6.59 \times 10^2 \pm 3.58 \times 10^2$

†Kato *et al.*¹⁰ Values shown as mean \pm SD.